SAND2017-11780PE

Exceptional service in the national interest

Sandia National Laboratories

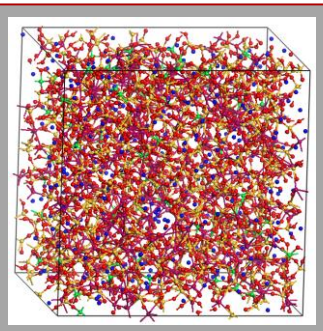
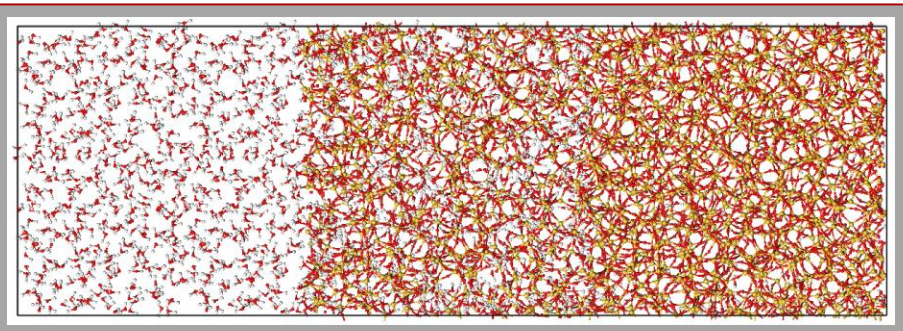
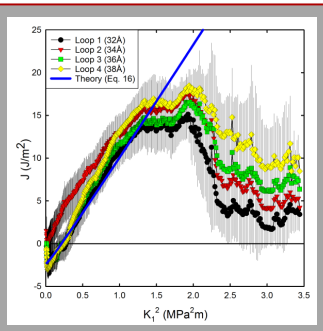

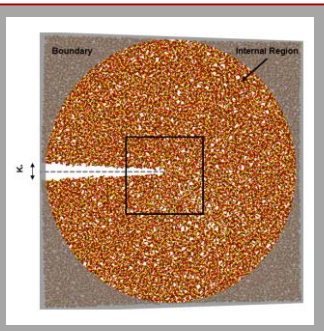

Dissolution and fracture properties of amorphous silica through classical molecular dynamics simulations

J.M. Rimsza

SNL: Louise Criscenti, Reese Jones
UNT: Jincheng Du, Jeffrey Kelber, Lu Deng
UNT/Lam Research: Haseeb Kazi, Frank Pasquale
Penn. St: Adri van Duin, Seung Ho, Jejoon Yun (U.C. Merced)

U.S. DEPARTMENT OF ENERGY | NNSA National Nuclear Security Administration

Sandia National Laboratories is a multi-mission laboratory managed and operated by National Technology and Engineering Solutions of Sandia, LLC., a wholly owned subsidiary of Honeywell International, Inc., for the U.S. Department of Energy's National Nuclear Security Administration under contract DE-NA0003525.

Outline

- Introduction
- Computational methods
- Silica glass dissolution
- Silica glass fracture
- Conclusions

Background

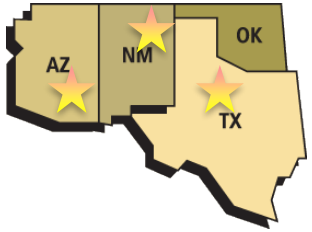

Sandia National Laboratories

THE UNIVERSITY OF ARIZONA

Tucson, AZ

UNT UNIVERSITY OF NORTH TEXAS

Denton, TX

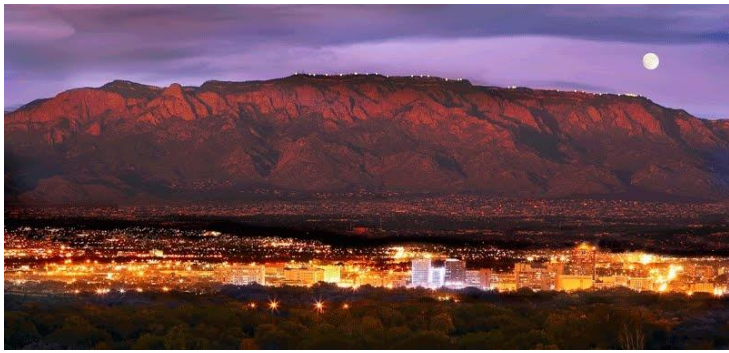

Sandia National Laboratories

Albuquerque, NM

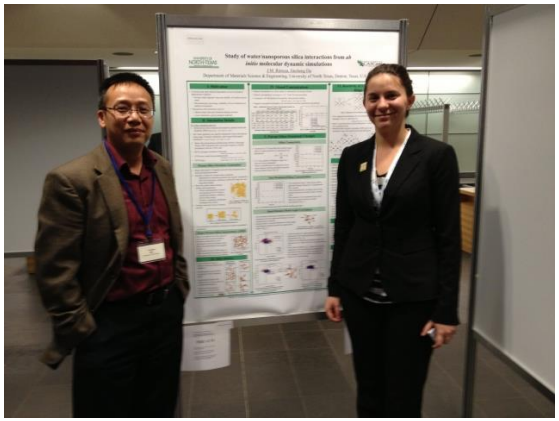

Molecular Modeling

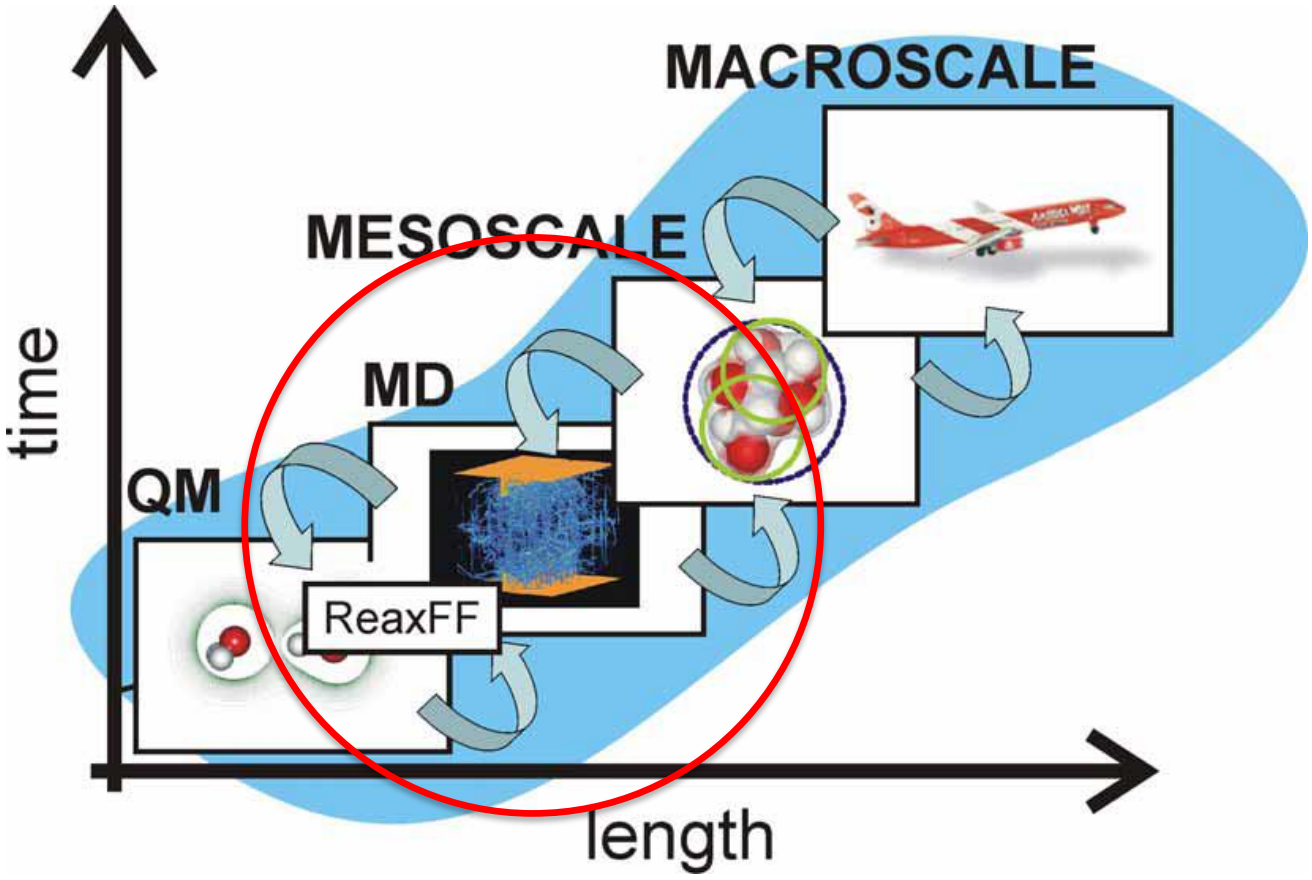

Markus J. Beuhler, Lecture, MIT . (2006).

Classical Molecular Dynamics

- Interatomic forces - Newtonian mechanics (based on position, velocity, force ect.)
- “Potential” describes molecular interactions: Lennard-Jones

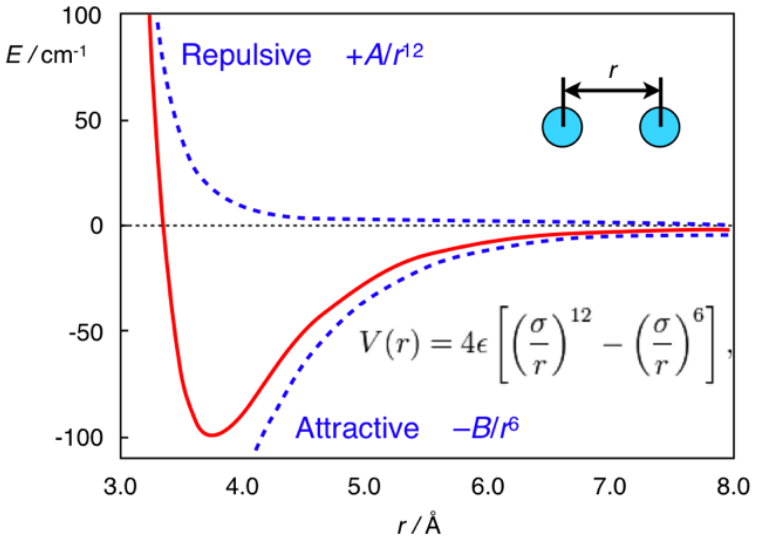

Jenna Rocca “Lennard Jones Potential Equation” June 24 2016

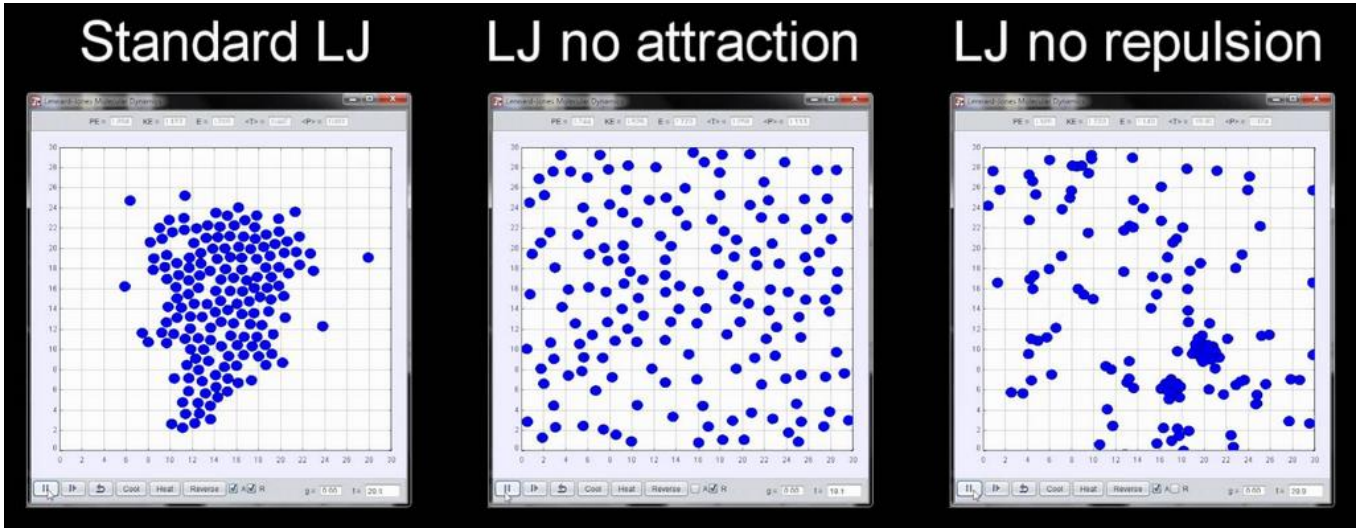

Weikang Sun “Modified Lennard-Jones Fluid Simulation with EJS” 2017

Classical Molecular Dynamics Forcefields

- Forcefield development is an “art” rather than a “science”
- Each group uses their preferred forcefield
- Results in numerous branching forcefields

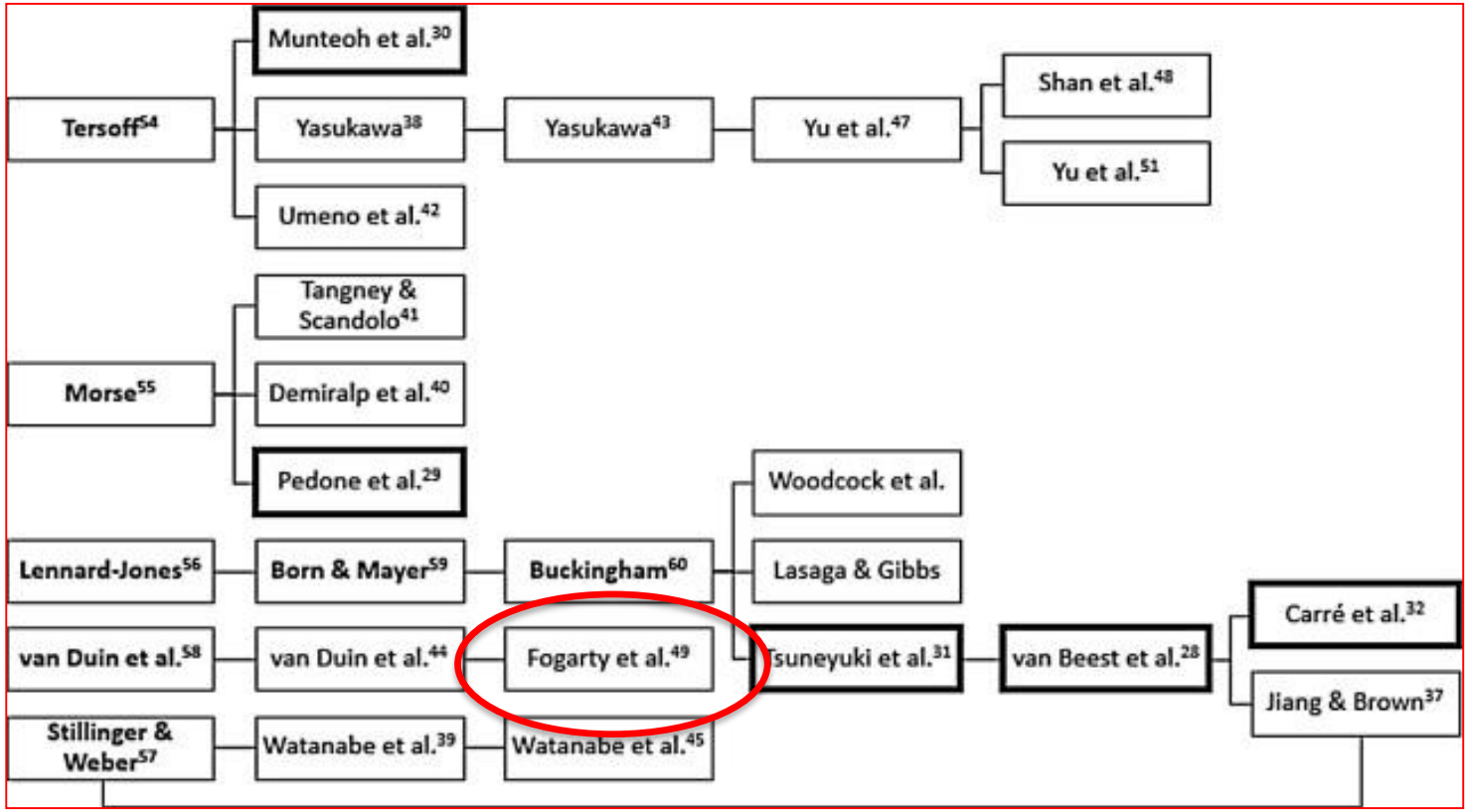

Soules, Thomas F., et al. *J. Non-Crys. solids* (2011)

ReaxFF Forcefield

Sandia National Laboratories

$$E_{\text{system}} = E_{\text{bond}} + E_{\text{over}} + E_{\text{under}} + E_{\text{val}} + E_{\text{pen}} + E_{\text{tors}} + E_{\text{conj}} + E_{\text{vdWaals}} + E_{\text{Coulomb}}$$

$$E_{\text{bond}} = -D_e \cdot \text{BO}_{ij} \cdot \exp[p_{\text{be},1}(1 - \text{BO}_{ij}^{p_{\text{be},1}})]$$

$$E_{\text{over}} = p_{\text{over}} \cdot \Delta_i \cdot \left(\frac{1}{1 + \exp(\lambda_6 \cdot \Delta_i)}\right)$$

$$E_{\text{under}} = -p_{\text{under}} \cdot \frac{1 - \exp(\lambda_7 \cdot \Delta_i)}{1 + \exp(-\lambda_8 \cdot \Delta_i)} \cdot f_6(\text{BO}_{ij,\pi}, \Delta_j)$$

$$E_{\text{val}} = f_7(\text{BO}_{ij}) \cdot f_7(\text{BO}_{jk}) \cdot f_8(\Delta_j) \cdot \{k_a - k_a \exp[-k_b(\Theta_o - \Theta_{ijk})^2]\}$$

$$E_{\text{pen}} = \lambda_{19} \cdot f_9(\Delta_j) \cdot \exp[-\lambda_{20} \cdot (\text{BO}_{ij} - 2)^2] \cdot \exp[-\lambda_{20} \cdot (\text{BO}_{jk} - 2)^2]$$

$$E_{\text{tors}} = f_{10}(\text{BO}_{ij}, \text{BO}_{jk}, \text{BO}_{kl}) \cdot \sin\Theta_{ijk} \cdot \sin\Theta_{jkl} \left[\frac{1}{2}V_2 \cdot \exp\{p_l(\text{BO}_{jk} - 3 + f_{11}(\Delta_j, \Delta_k))^2\} \cdot (1 - \cos 2\omega_{ijkl}) + \frac{1}{2}V_3 \cdot (1 + \cos 3\omega_{ijkl})\right] \quad (10a)$$

$$E_{\text{conj}} = f_{12}(\text{BO}_{ij}, \text{BO}_{jk}, \text{BO}_{kl}) \cdot \lambda_{26} \cdot [1 + (\cos^2 \omega_{ijkl} - 1) \cdot \sin\Theta_{ijk} \cdot \sin\Theta_{jkl}]$$

$$E_{\text{vdWaals}} = D_{ij} \cdot \left\{\exp\left[\alpha_{ij} \cdot \left(1 - \frac{f_{13}(r_{ij})}{r_{\text{vdW}}}\right)\right] - 2 \cdot \exp\left[\frac{1}{2} \cdot \alpha_{ij} \cdot \left(1 - \frac{f_{13}(r_{ij})}{r_{\text{vdW}}}\right)\right]\right\}$$

$$E_{\text{Coulomb}} = C \cdot \frac{q_i \cdot q_j}{[r_{ij}^3 + (1/\gamma_{ij})^3]^{1/3}}$$

Van Duin, Adri CT, et al. "ReaxFF: a reactive force field for hydrocarbons." *The Journal of Physical Chemistry A* 105.41 (2001): 9396-9409.

ReaxFF Applications

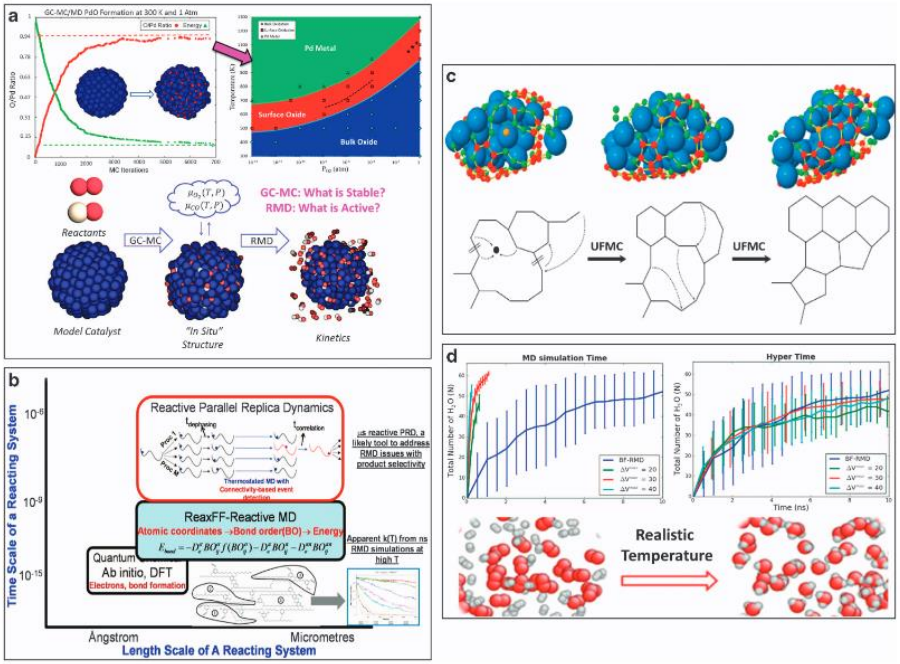

New simulation techniques for the ReaxFF potential: (a) grand canonical Monte Carlo, (b) parallel replica dynamics, (c) uniform-acceptance force-biased Monte Carlo, and (d) adaptive accelerated molecular dynamics.

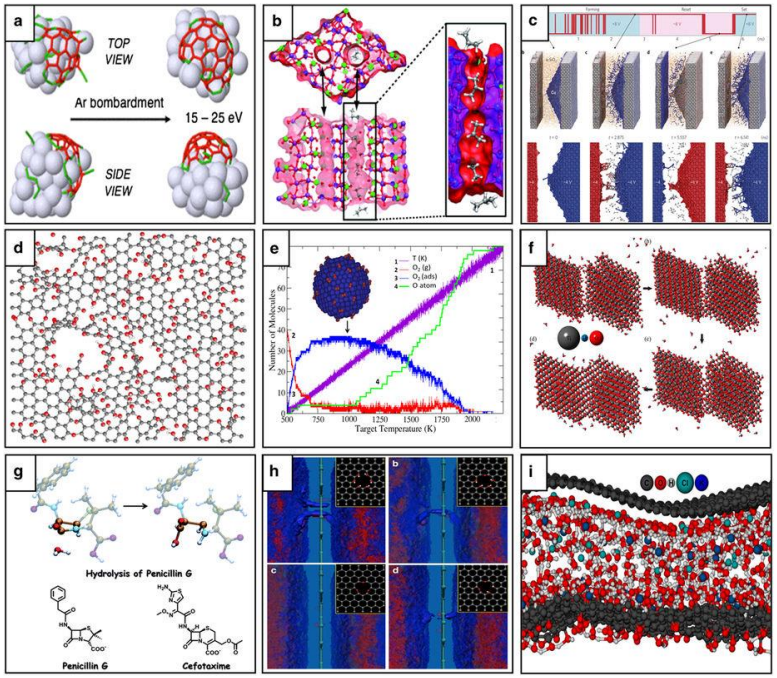

Application of the ReaxFF method to (**a**) Ni-catalysed CNT growth, (**b**) oxidative dehydrogenation over MMO catalysts, (**c**) electrometallisation cells, (**d**) reduction of graphene oxide, (**e**) Pd surface oxidation, (**f**) oriented attachment mechanisms in TiO_2 nanocrystals, (**g**) conformational dynamics of biomolecules, (**h**) proton diffusion membranes and (**i**) capacitive mixing by double layer expansion.

Senftle, Thomas P., et al. "The ReaxFF reactive force-field: development, applications and future directions." *npj Computational Materials* 2 (2016): 15011.

Dissolution of Amorphous Silica

Jessica M. Rimsza (Sandia National Laboratories)

Co-Authors: Jincheng Du (UNT), Jeffrey Kelber (UNT), Lu Deng (UNT), Haseeb Kazi, (UNT, Lam Research), Adri van Duin (Penn. St.), Jejoon Yun (Penn. St., U.C. Merced)

Funding: This work was supported through the DOE Nuclear Energy University Partnership (NEUP) and the NSF Graduate Research Fellowship Program (GRFP)

Vitrification of nuclear waste glasses

- How to store nuclear waste without impacting the environment?
- Vitrification - immobilize nuclear waste in a stable amorphous network
- Composition: borosilicate glasses

Liquid nuclear waste in barrels

Vitrified nuclear waste

Table 1: International simple glass (ISG) and SON68 nuclear waste glasses compositions *Gin et al. Materials Today (2013)*

Composition (Mole %)	SiO_2	B_2O_3	Na_2O	Al_2O_3	CaO	ZrO_2	Other
ISG	60.2	16.0	12.6	3.8	5.7	1.7	0.0
SON68	45.5	14.0	9.9	4.9	4.0	2.7	19.0*

*Other elements: Li_2O, Fe_2O_3, P_2O_5, NiO, Cr_2O_3, Cs_2O, SrO, Y_2O_3, MoO_3, MnO_2, CoO, Ag_2O, CdO, SnO_2, Sb_2O_3, TeO_2, BaO, La_2O_3, Ce_2O_3, Pr_2O_3, Nd_2O_3, UO_2, and ThO_2

Hanford Plant, Washington state

What are the mechanisms and processes which govern the dissolution of silicate glasses in aqueous environments?

Images: http://www.hanfordvitplant.com/about-project http://www.hanford.gov/page.cfm/AdvancesinGlassChemistry https://www.sheffield.ac.uk/news/nr/nuclear-waste-storage-glass-sheffield-1.203561

Stages of glass dissolution

1. Interdiffusion between water and network modifiers
2. Hydrolysis of Si-O-Si bonds
3. Formation of a protective layer
4. Development of a residual dissolution rate
5. Precipitation of large silicate minerals

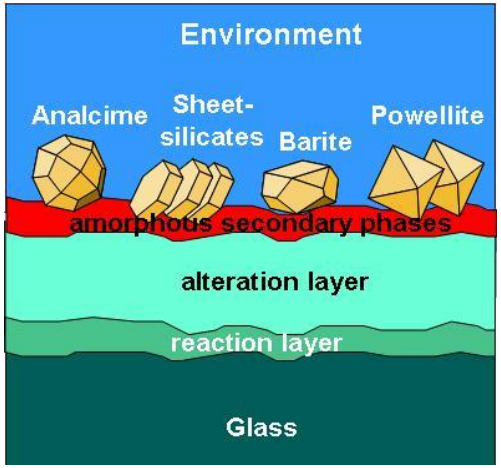

https://www.ine.kit.edu/english/417.php

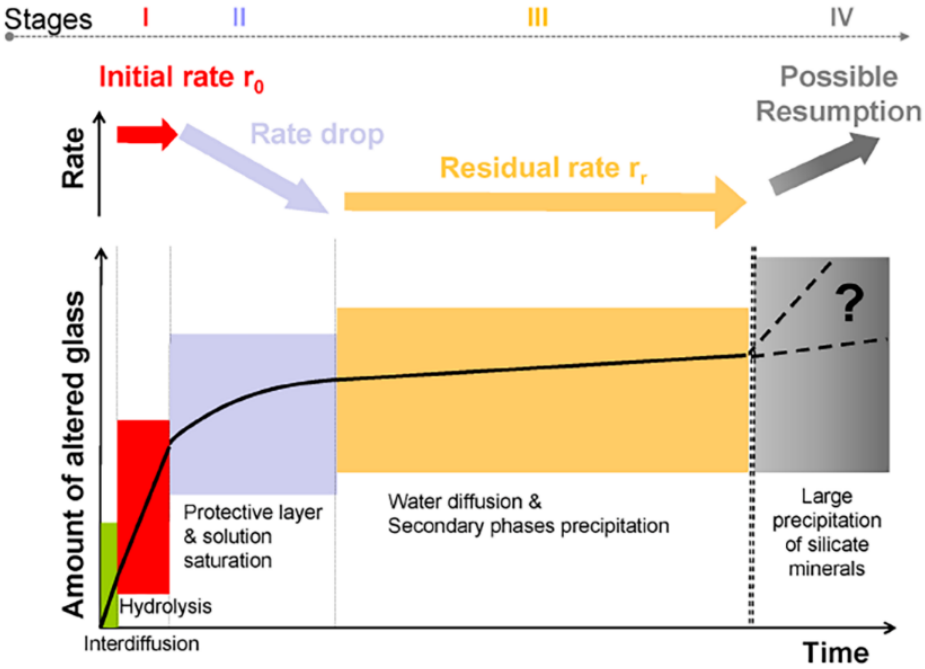

Gin et al. Procedia Mat. Sci. (2014)

Silica gel alteration layer

Silica gel alteration layer affects the dissolution rate due to:

- Slowing water diffusion
- Acting as a molecular sieve
- Providing more reactive sites for water
- Re-polymierizing silica from solution

Development of silica-gel-water (SGW) model structure

- Begins with a dense silica structure
- ½ becomes the dense silica region and ½ is the silica gel
- 400 of the 1000 silica in the gel region are removed
- Non-bridging oxygen are hydrogen terminated
- Structure is hydrated and bulk water region is added
- Forms a three component model consisting of silica-gel-water and silica-gel and gel-water interfaces

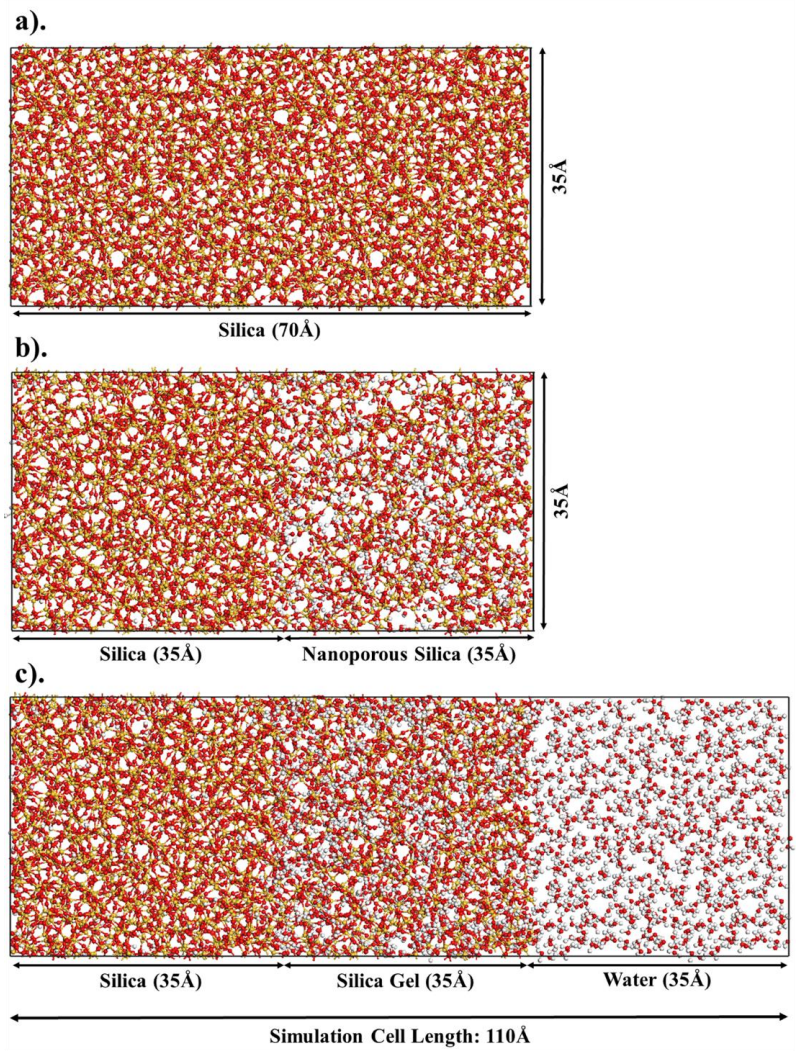

Schematic of the creation of a silica-gel-water (SGW) dissolution model

Simulation details

- High temperature simulation for structural evolution
- 1 ns of simulation with a 0.25 fs time step at 300K, 500K, 700K, or 900K
- After high temperature simulation temperature was decreased to 300K for 30ps
- Low temperature simulations:
  - Deconvolution of high temperature structures
  - Standardize analysis of the structure

Model number and temperature for 1 ns simulation

Model	Initial	SGW-1	SGW-2	SGW-3	SGW-4
Temperature (K)	N/A	300K	500K	700K	900K

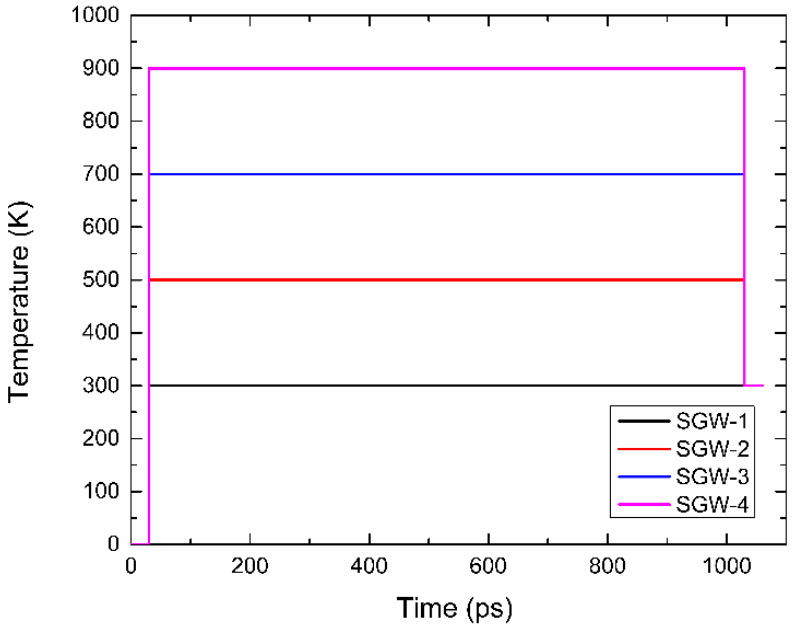

Changing temperature with time for the four different SGW model structures.

SGW model structure: simulated at 900K

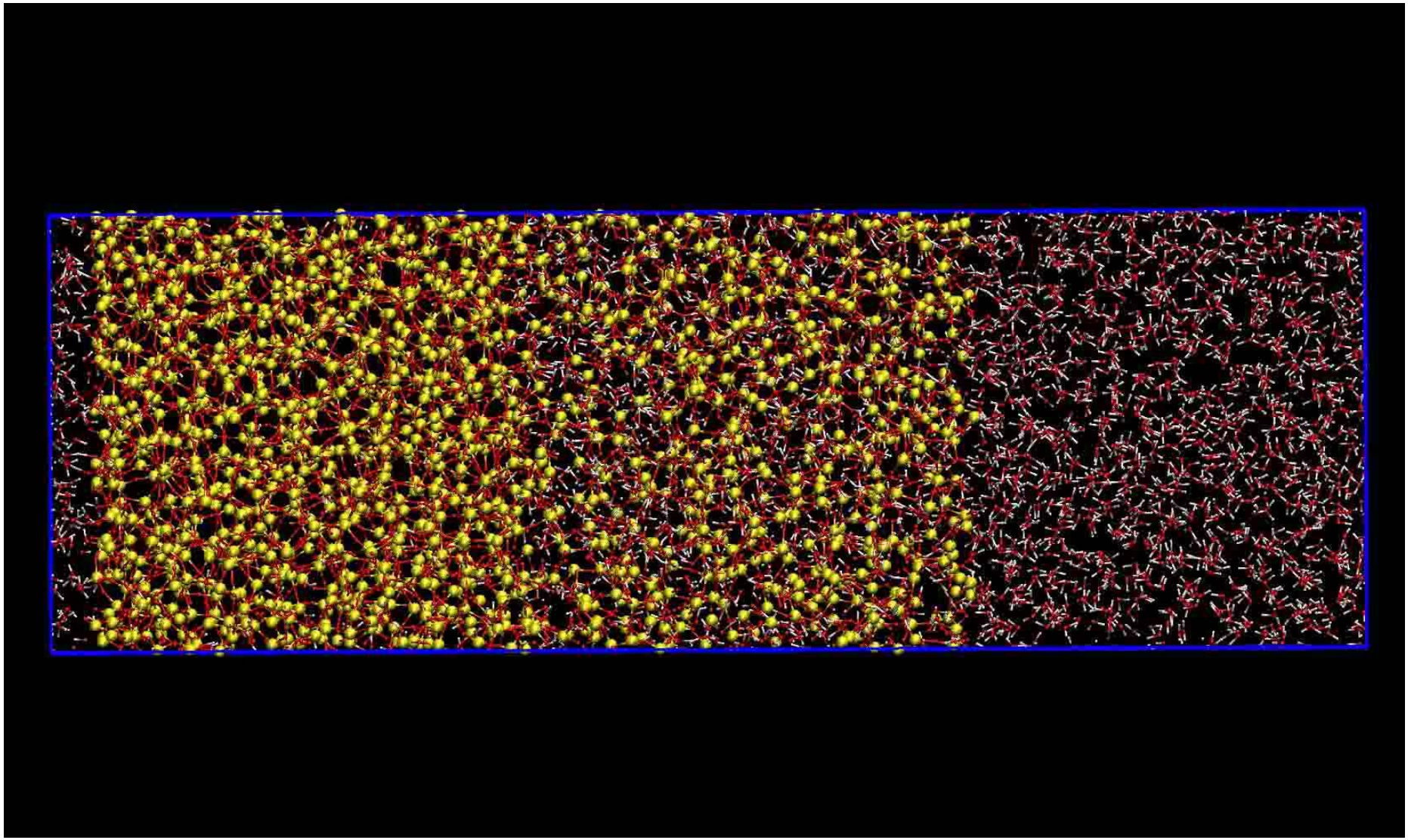

1 ns classical MD simulation of the SGW model at 900K

Growth of silica-gel-water regions

- Silica gel grows into the water region
- Gel-water interfaces thicken
- Silica and silica-gel regions remain stable

Silica density cut-off values for different regions

Region	Silica Cut-off (g/cm^3)
Silica	2.0
Gel	0.9
Water	0.2

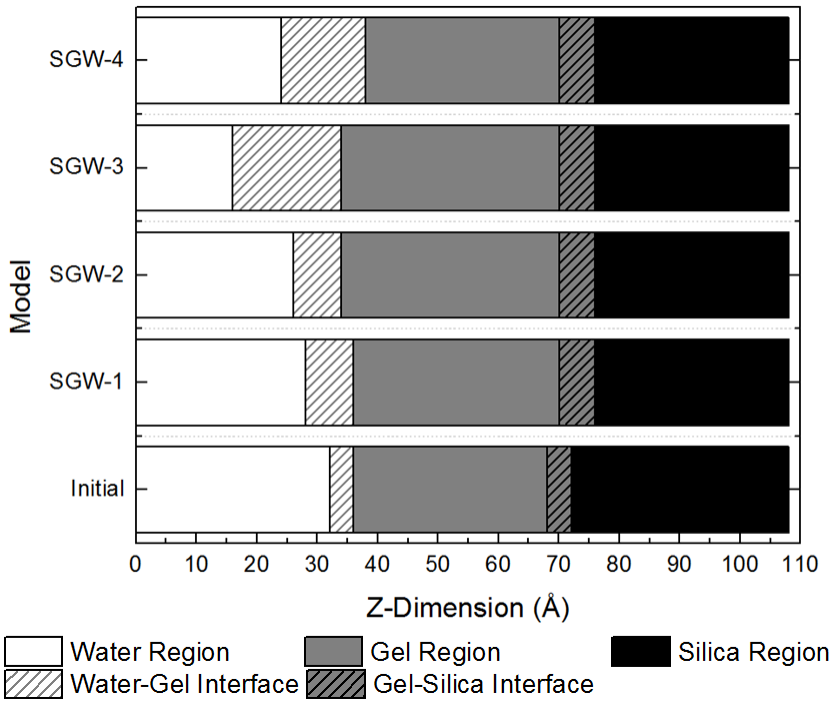

Schematic outline of width of the silica, gel, and water regions

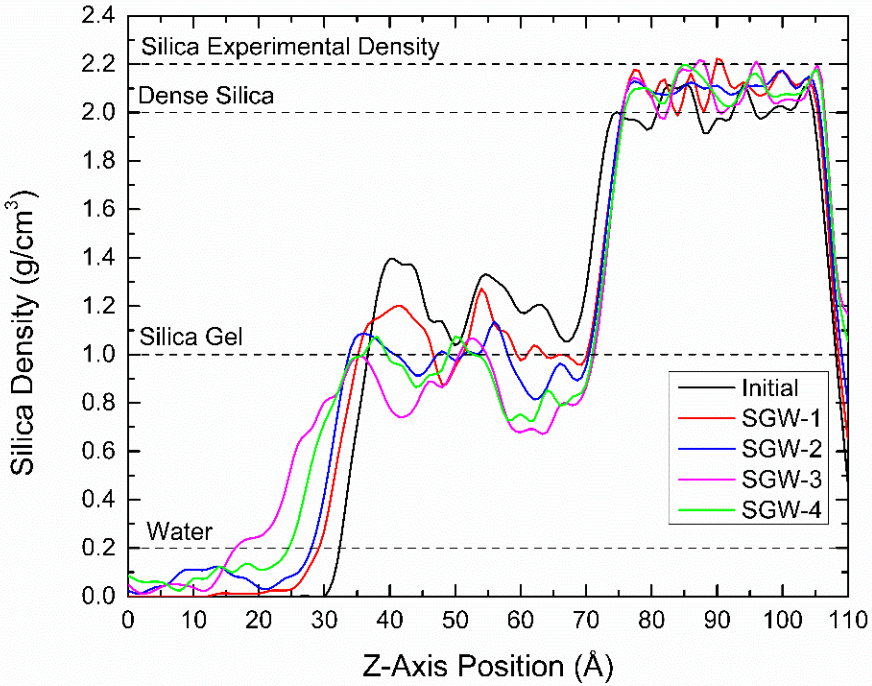

Z-density profile of silica density in SGW models

Q_n distribution of the silica gel

- Stability of Si-O bonds in SiO_4 tetrahedron is affected by the number of bridging oxygen
- Dissolution occurs with the conversion of $Q_4 \rightarrow Q_3 \rightarrow Q_2 \rightarrow Q_1 \rightarrow Q_0$ species in a step-wise fashion

Kagan and Garofalini. Phys. Chem. Chem. Phys. (2014)

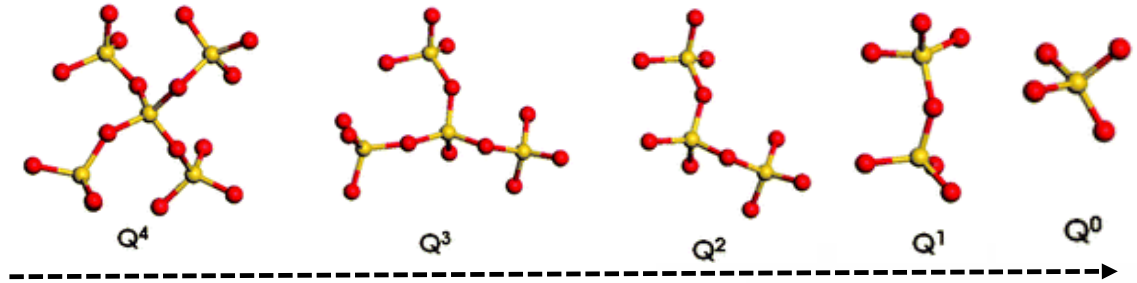

Chaprentier et al. RSC Adv. (2013)

- Highest energy barriers have been reported for the $Q_3 \rightarrow Q_2$ and $Q_2 \rightarrow Q_1$ transitions

Kagan and Garofalini. Phys. Chem. Chem. Phys. (2014)
Criscenti et al. J. of Phys. Chem. C (2006)

- Silica gel Q_n distribution:
  - Increases in Q_2, Q_3, and Q_4, concentrations
  - Decreases in Q_0 and Q_1 species
- Lower Q_n species are dissolved into the bulk water, increasing in higher Q_n species in the gel

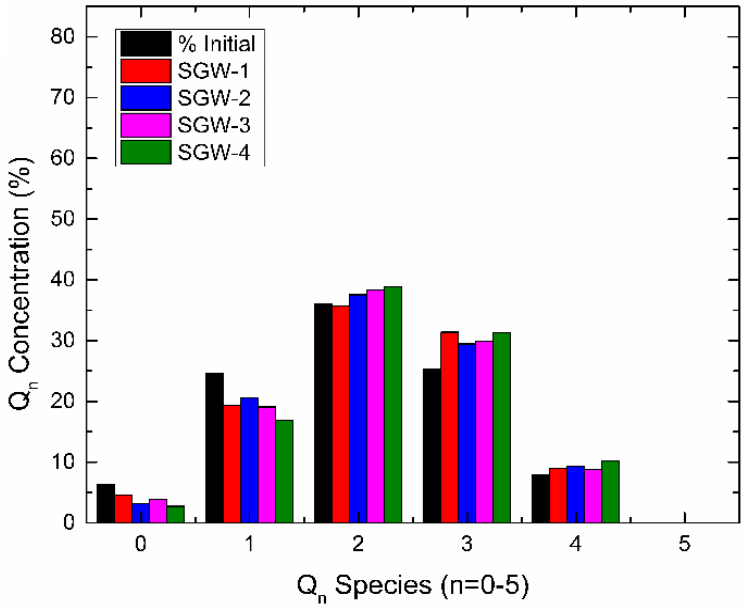

Q_n distribution of the gel region of the SGW models.

Ring size distribution of silica gel

- Initial gel structure has a fragmented ring structure
- After evolution the five-membered, six-membered, and seven-membered rings concentrations increase
- Trends toward the distribution seen in bulk silica
- Over time, would a silica backbone structure similar to dense silica form?

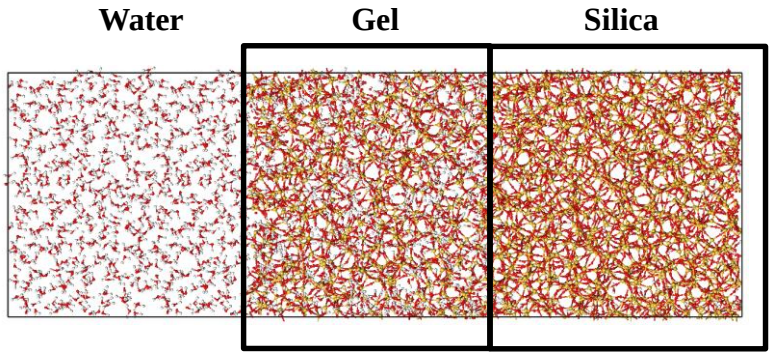

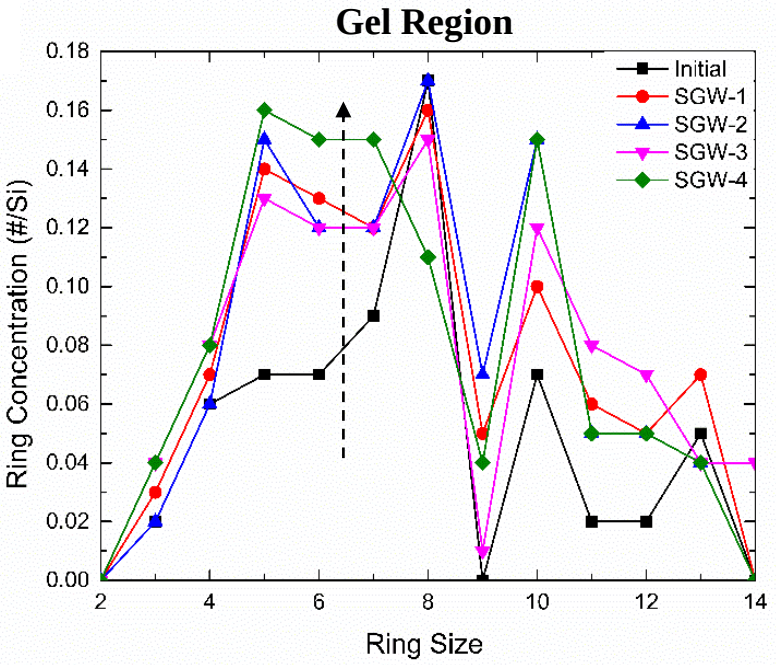

Ring size distribution of the gel region of the SGW model

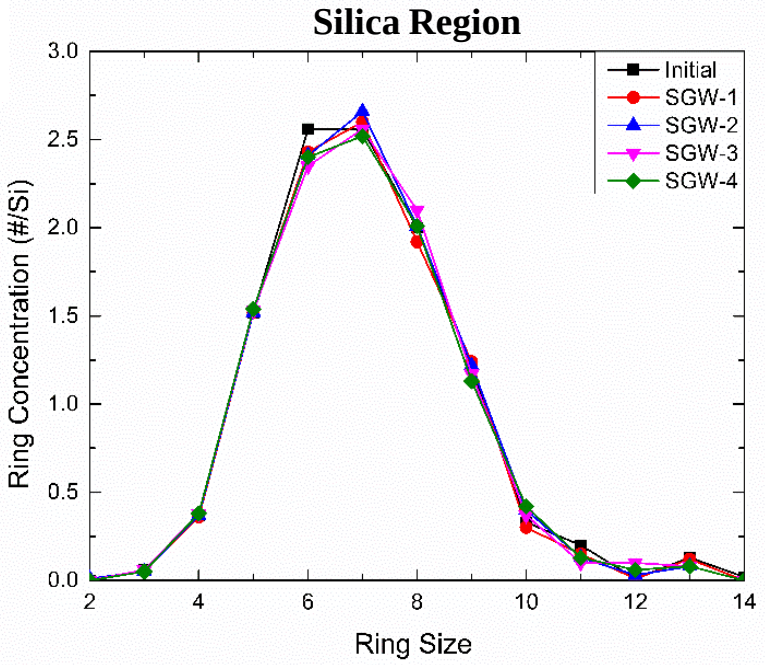

Ring size distribution of the silica region of the SGW model

Concentration of dissolved silica

- Primarily silica monomers occur in water (Raman spectroscopy) *Gunnarsson et al. Geochim. Cosmochim. Acta. (2000)*
- Water region: 50%+ silica monomers
- Silica concentration is higher than in experiments (1.5 g/L for pure amorphous silica at 300K)
  Dolstsinis et al. J. of Theo. Comp. Chem. (2007)
- Monomeric silica consistently increases with evolution of the structure

Dissolved silica in the water region

	All Si (g/L)	Monomers (g/L)
Initial	0.00±0.00	0.00±0.00
SGW-1	4.94±1.73	3.47±0.87
SGW-2	31.89±4.65	8.77±1.65
SGW-3	19.71±3.57	11.00±1.87
SGW-4	40.49±4.44	11.90±1.93

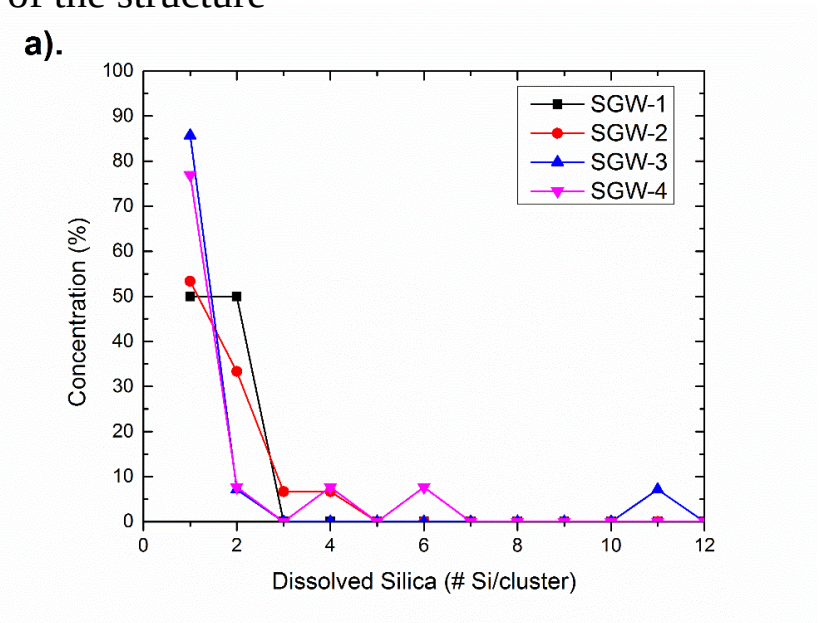

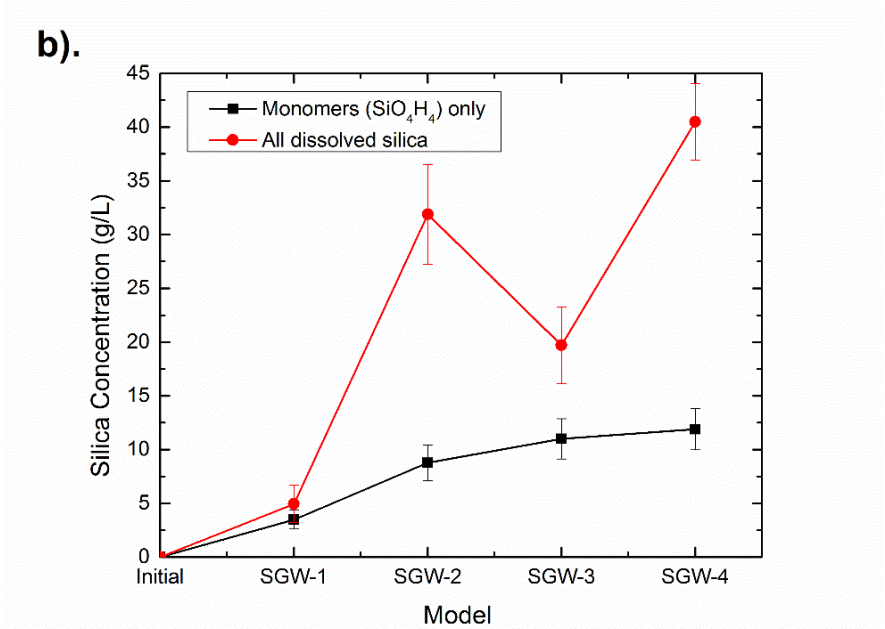

(a) Dissolved silica concentration in the SGW models as either monomers or larger silica polymer chains, and (b) distribution of dissolved silica molecules by the number of silicon atoms in a cluster.

Related work

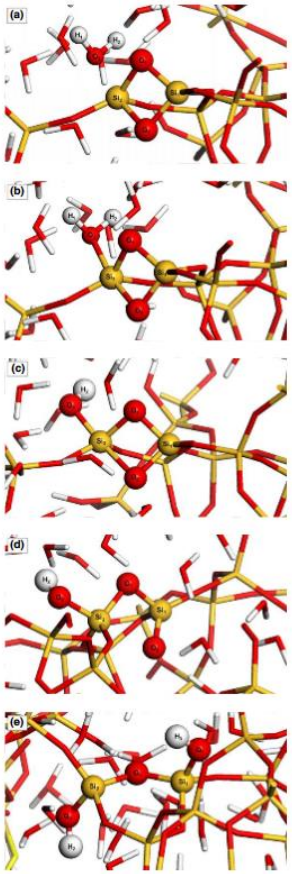

Fig. 2. Snapshots of the five representing steps of the mechanism of two-membered ring breakage in a 60% nanoporous silica system in the presence of water.

Rimsza, J. M., and J. Du. *J. Amer. Ceram. Soc.* 98.12 (2015): 3748-3757.

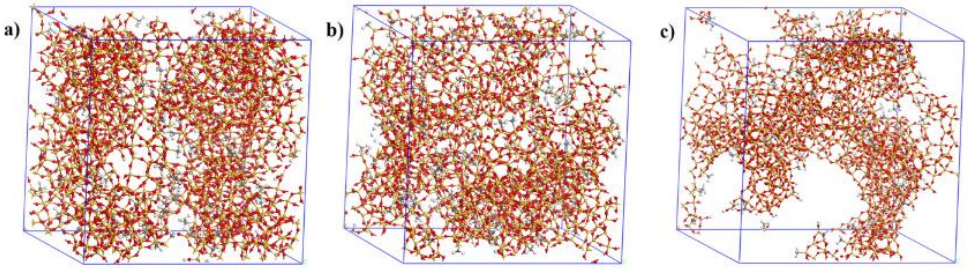

Fig. 3. Simulated nanoporous OSG structures using ReaxFF for the lattice expansion (LE) method at a) 32.94%, b) 46.29%, and c) 73.08% porosity. The red is the oxygen atoms and the yellow is silicon.

Rimsza, J. M., L. Deng, and J. Du. *J. Non-Crys. Solids* 431 (2016): 103-111.

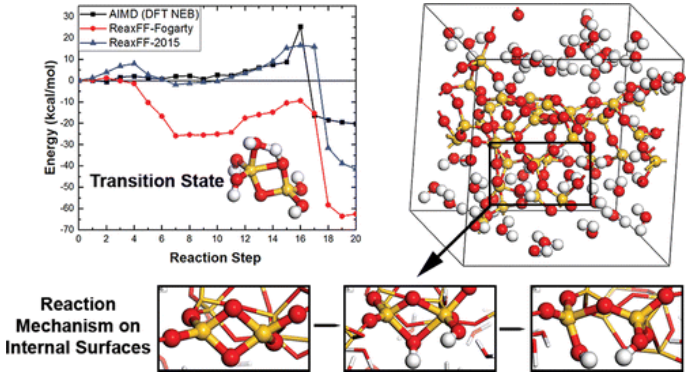

Rimsza, J. M., et al. *J. Phys. Chem. C* 120.43 (2016): 24803-24816.

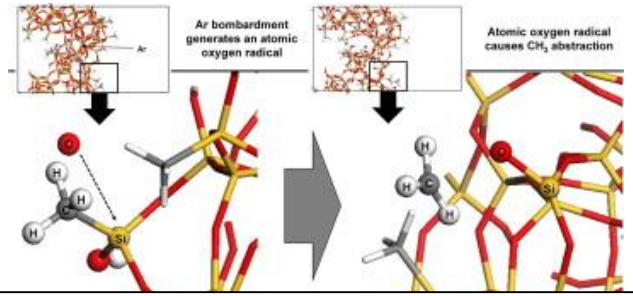

Rimsza, J. M., and J. Du. *Comput. Mater. Sci.* 110 (2015): 287-294.

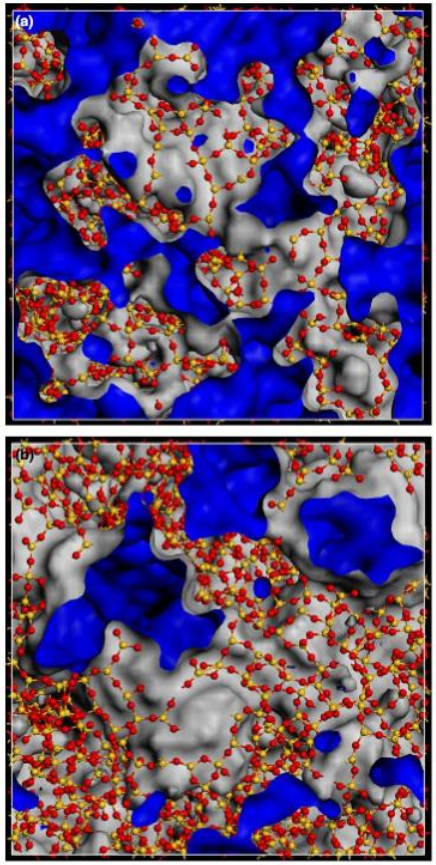

Fig. 2. Snapshot of the cross-section views of porous silica structures developed with the (a) volume scaling and (b) charge scaling simulation methods with around 42% porosity. Yellow atoms are silicon, red atoms are oxygen, and the Connolly surface (as described in section II) is outlined in blue (internal surface) and gray (external surface). The simulation cell size of (a) is 42.79 A.× 42.79 A × 42.79 A and that for (b) is 42.88 A × 42.88 A × 42.88 A.

Rimsza, J. M., and J. Du. *J. Amer. Ceram. Soc.* 97.3 (2014): 772-781.

Fracture of Amorphous Silica

Jessica M. Rimsza (Sandia National Laboratories)

Co-Authors: Louise Criscenti (SNL), Reese Jones (SNL), Adri van Duin (Penn. St.), Seung Ho (Penn. St.)

This work was fully supported by the Laboratory Directed Research and Development (LDRD) program of Sandia National Laboratories.

Technical motivation

Natural systems: hydrocracking, carbon sequestration

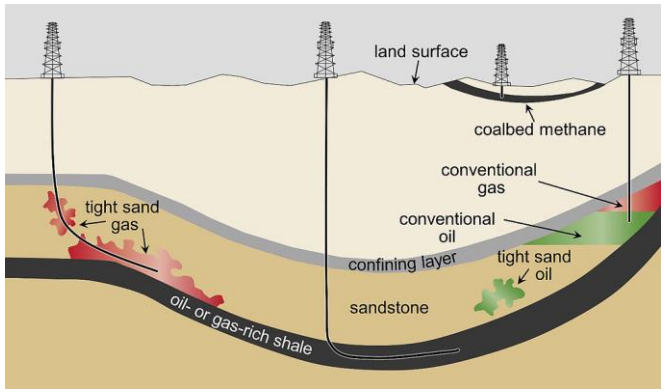

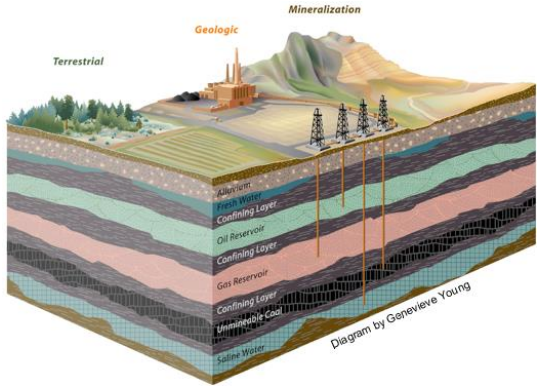

Engineered systems: nuclear glass waste forms, glass-to-metal hermetic seals

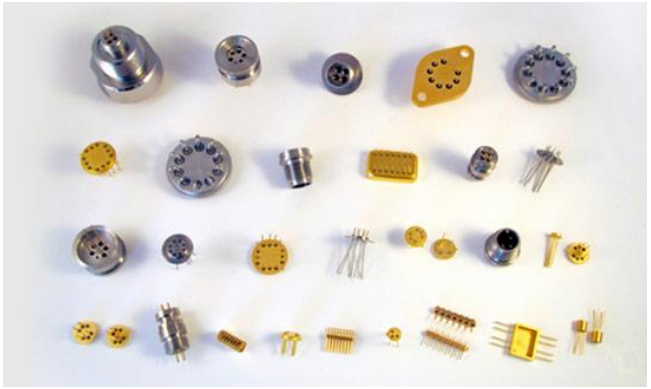

Image References: *http://wikivisually.com/wiki/Fracking, http://co2.egi.utah.edu/, https://eesa.lbl.gov/projects/waste-form-degradation-modeling/ , http://www.completehermetics.com/glass-to-metal-seals-and-feedthroughs/*

Introduction to fracture mechanics

- Cracks propagate when the stress at the crack tip exceeds the strength of the material (Griffith criterion)

$$\sigma = \left(\frac{2E\gamma}{\pi a}\right)^{\frac{1}{2}}$$

A.A. Griffith, Phil. Trans. R. Soc. A (1921)

- Fracture toughness (K): the energy required to propagate a crack in a material

- Strain energy release rate (G): energy dissipated during fracture per unit of surface area

$$G = \frac{K_c^2(1-\nu)^2}{E} = 2\gamma_s \qquad \text{(brittle material)}$$

$$G = G_{diss} + 2\gamma_s \qquad \text{(material with inelastic behavior)}$$

- J-integral: method of calculating G for monotonic loading through a path independent contour integral
  - For a linear elastic (non-yielding) material G=J
  - Bulk material property
  - In Mode I: $J_{IC} = G_{IC} = K_{IC}^2\left(\frac{1-\nu^2}{E}\right)$
    - E: elastic modulus
    - ν: poission's ratio
- Modes of loading
  - Mode 1: Opening
  - Mode 2: Sliding
  - More 3: Tearing

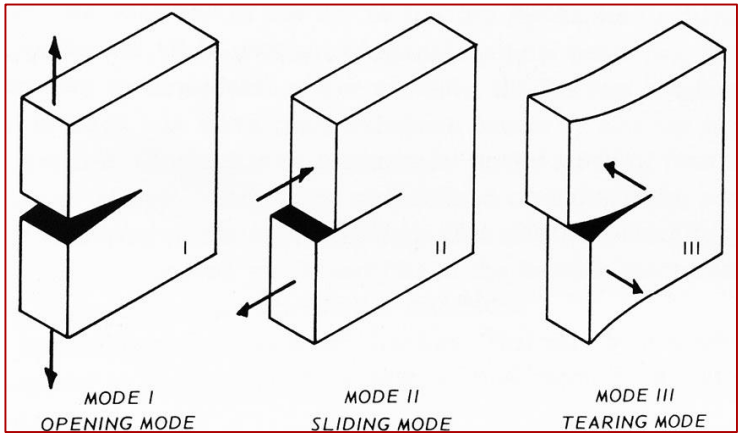

http://thediagram.com/12_3/thethreemodes.html

Zhu, X, and J.A. Joyce. Eng. Fract. Mech. (2012)

Computational methods

- J-integral and the fracture toughness calculated from stress, displacement and energy densities of atomistic system coarse grained onto a grid

Jones, Reese E., et al. *J. Phys.: Condens. Matter* (2010)

- Eshelby stress (S) is calculated and the J-integral is evaluated around a loop around the crack tip
- Atoms-to-Continuum (ATC) package calculates the J-integral and the fracture toughness from atomic stresses and is available as a USER-ATC LAMMPS Package

$$J = \int_{\partial\Omega} S \cdot dA$$

- Slit crack created forming a high stress condition
- Far-field loading through fixed boundary atoms with mode I stress
- Stress is introduced iteratively byincreasing the crack width

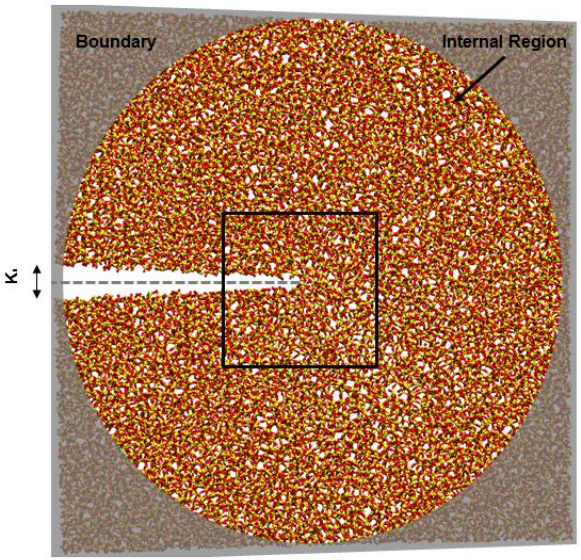

Schematic of silica slit crack, crack width, as well as boundary and internal regions. Atoms: oxygen (red), silicon (yellow)

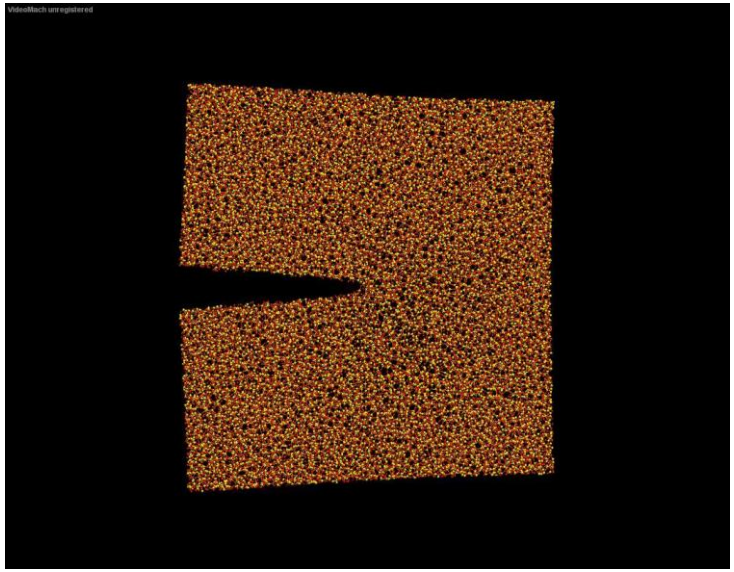

Opening of silica slit crack
Atoms: oxygen (red), silicon (yellow)

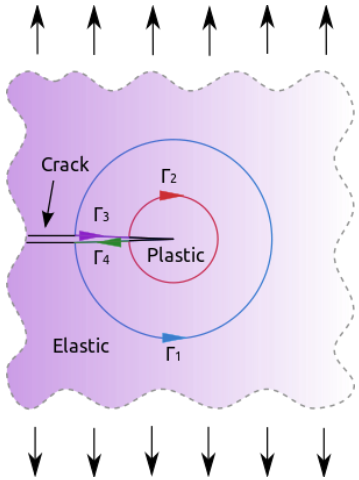

Bhanerje, "J-integral contours for an elastic material" 9/4/2013

Schematic of J-integral demonstrating the inclusion of the plastic region inside an elastically responding matrix

Fracture and energy dissipation

- Fracture propagates in distinct steps
- Perfectly brittle fracture will have no dissipation energy, with all energy used to propagate the fracture
- Dissipation energy calculated from the total energy of the system and added surface energy

$$\frac{\Delta U}{\Delta S_A} = G_{diss}$$

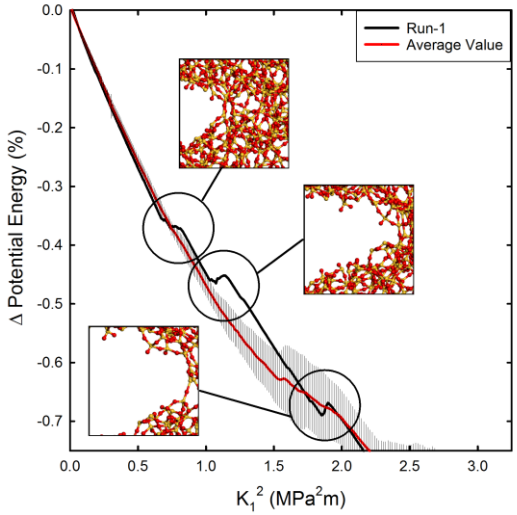

Potential energy change with loading for a single simulation (Run-1) and averaged

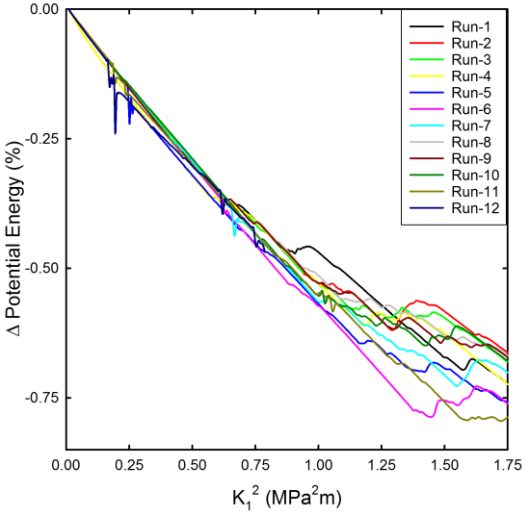

Potential energy change for individual simulations with loading of 0-1.75 K_I^2 (MPa^2m)

- Local inelastic behavior is introduced into the matrix during loading and not completely dissipated once fracture occurs

$$G = 2\gamma_s + G_{diss}$$

- Surface energies (γ_s): 2-1.2 J/m^2 varying with surface structure and relaxation

Rimsza, J. M. et al. *Langmuir* (2017).

Estimated G values are ~5.9-7.5 J/m^2

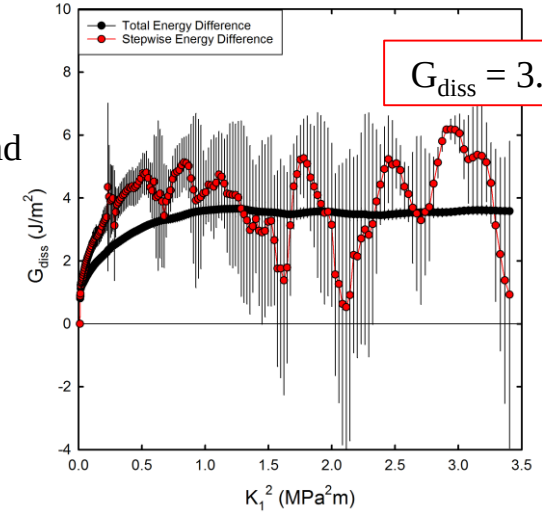

Energy dissipation (G_{diss}) during loading and subsequent crack propagation in amorphous silica

J-integral calculation

- Calculated via the AtC method through coarse graining energy, displacement, and stress
  Jones, Reese E., et al. *J. Phys.: Condens. Matter* (2010)
- J_{IC} value = J-integral when the crack begins propagating

$$J_{IC} = \frac{K_{IC}^2}{E^*} \qquad E^* = \frac{2\mu}{1-\nu}$$

- J-integral converges at loop sizes of ~3 nm approximates the size of an inelastic zone

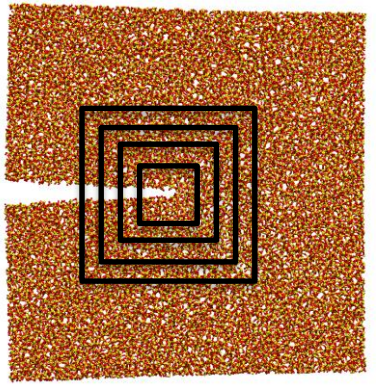

Schematic of increasing loop sizes for J-integral convergence test

K_{IC}=0.76±0.16 MPa√m
J_{IC}=6.16±4.34 J/m^2

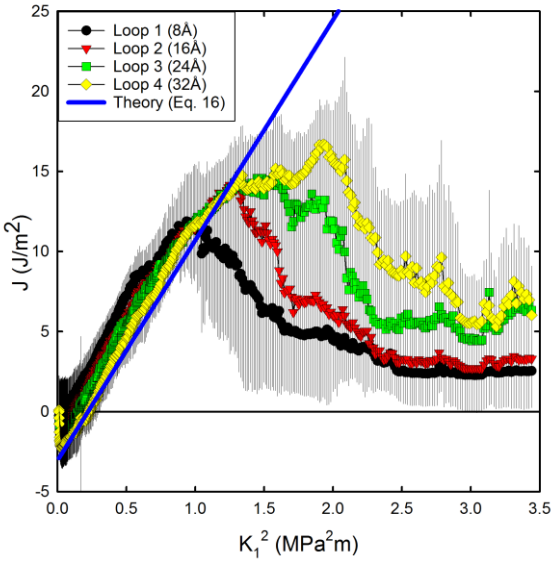

J-integral with increasing loop sizes

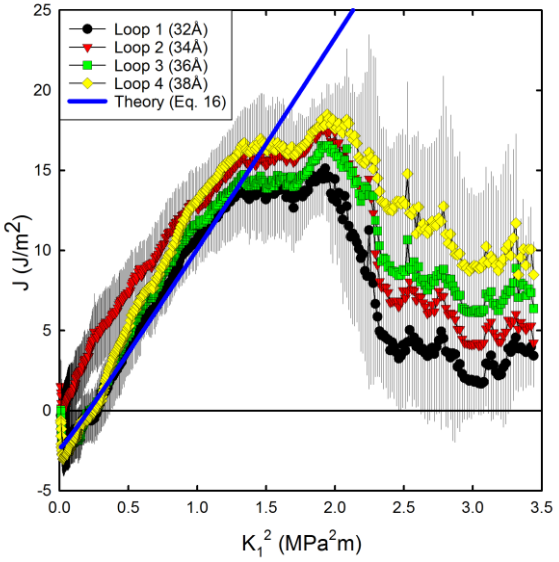

J-integrals with converged loop sizes

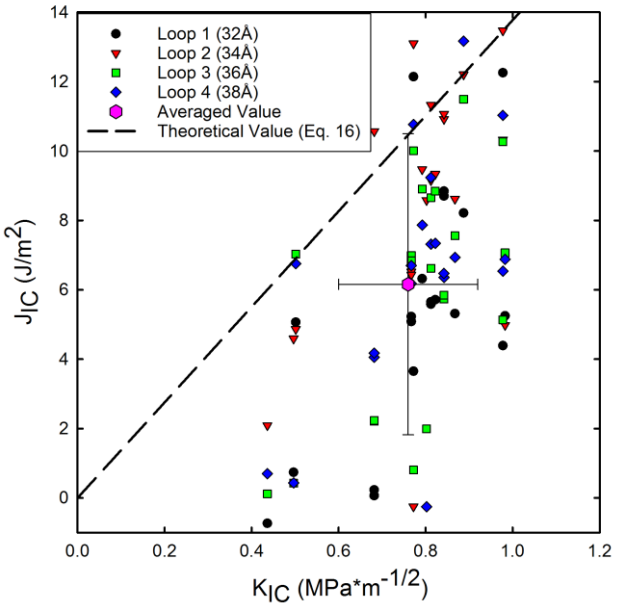

K_{IC} and J_{IC} values for the initiation of crack propagation in amorphous silica

Fracture: aqueous conditions

- Coupled chemical-mechanical processes inside the crack increases crack velocity in silicates
- Environmental effects are responsible for “subcritical fracture”, crack propagation at lower fracture toughness
- Due to reaction of water molecules at the crack tip

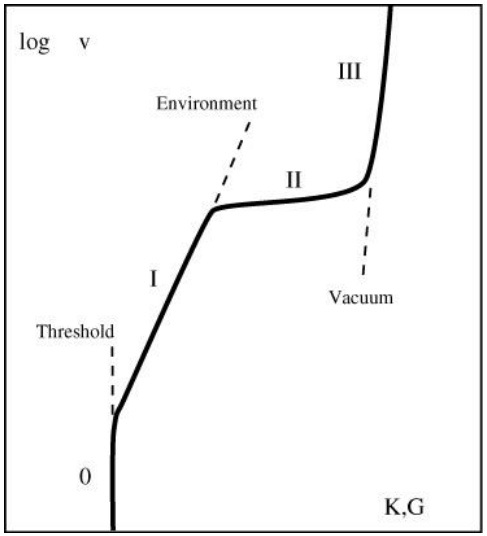

Ciccotti, Matteo *J. Phys. D: Appl. Phys.* (2009)

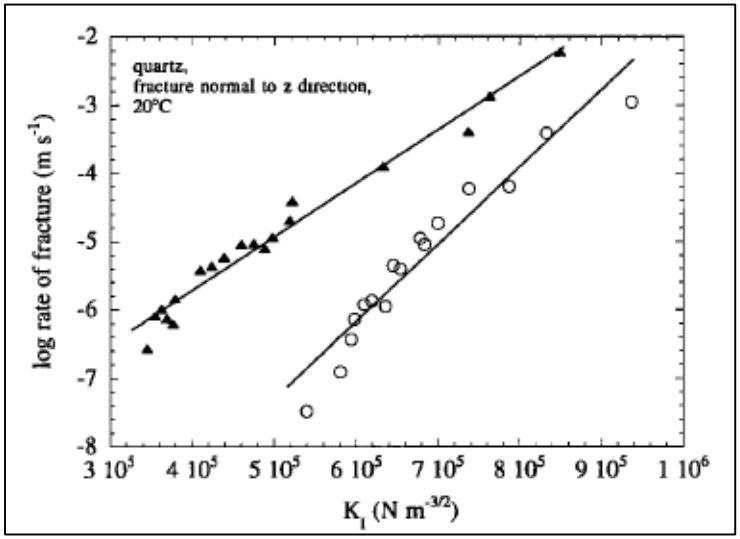

P.M. Dove, *J. Geophys. Res.* (1995)

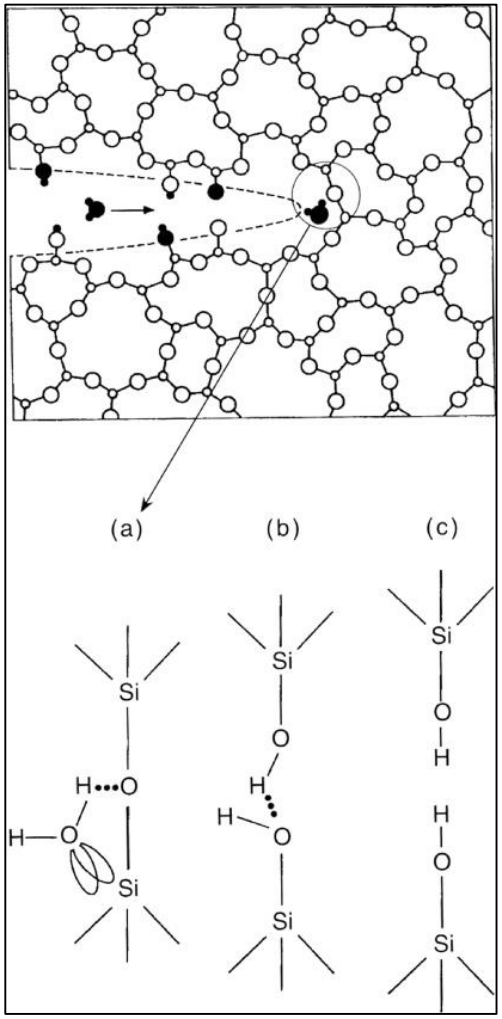

Ciccotti, Matteo *J. Phys. D: Appl. Phys.* (2009)

Computational methods

Introduce thin film of water which wets the crack surfaces

Water molecules added via GCMC to maintain surface wetting

Vary the fluid composition to investigate the effect of dissolved salts on fracture (dissolved NaCl, pH)

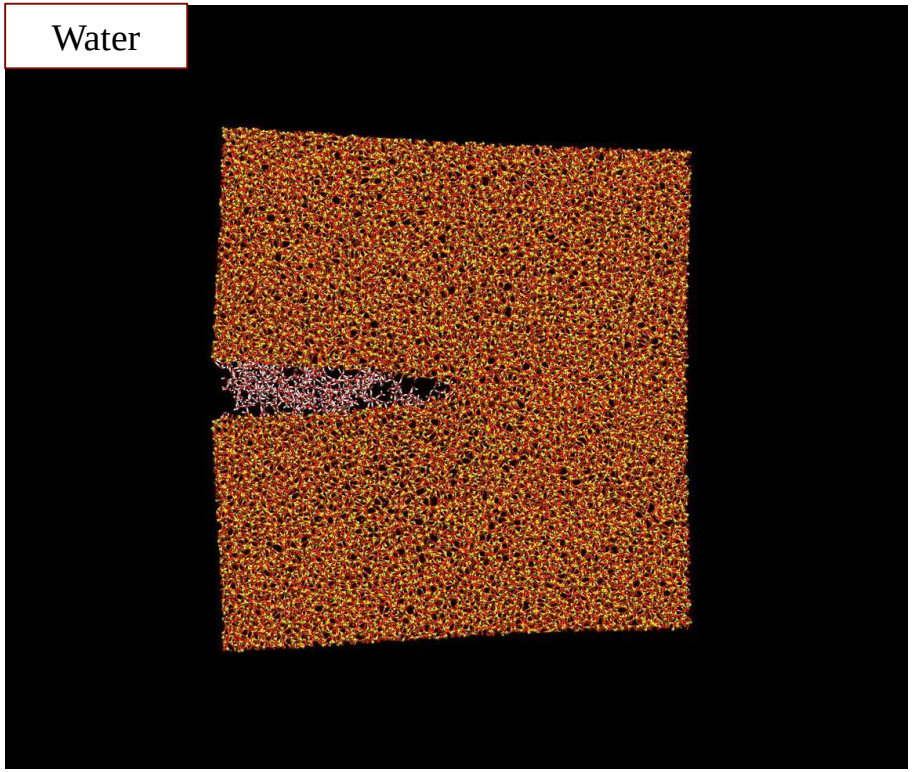

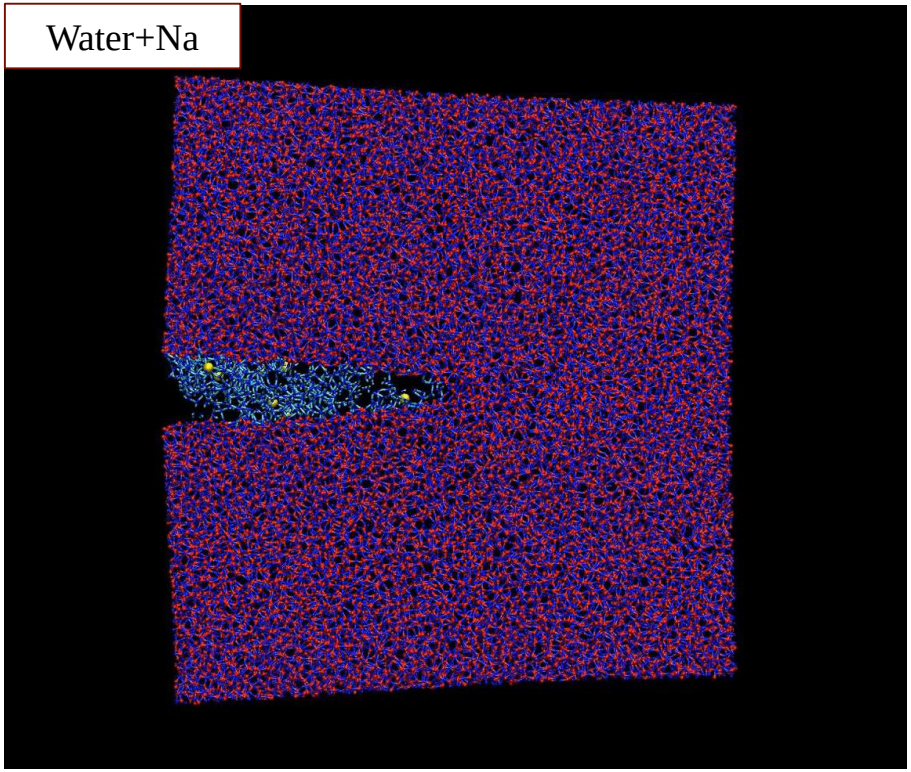

Opening of silica slit crack in a hydrated environment
Atoms: oxygen (red), silicon (purple), hydrogen (blue), sodium (yellow)

Bond concentration and connectivity

- Bond concentration:
  - Environment alters rate of bond breakage and formation
  - Increased Si-O bond breakage in water and water+sodium hydroxide systems
  - Investigation of statistical variation of fracture with different environments is ongoing

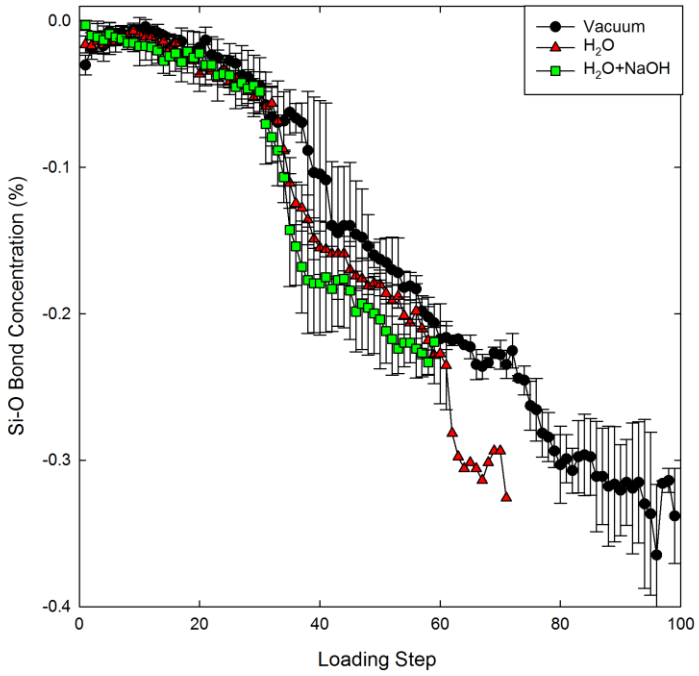

Si-O bond concentration of the system with loading for silica in three different environments

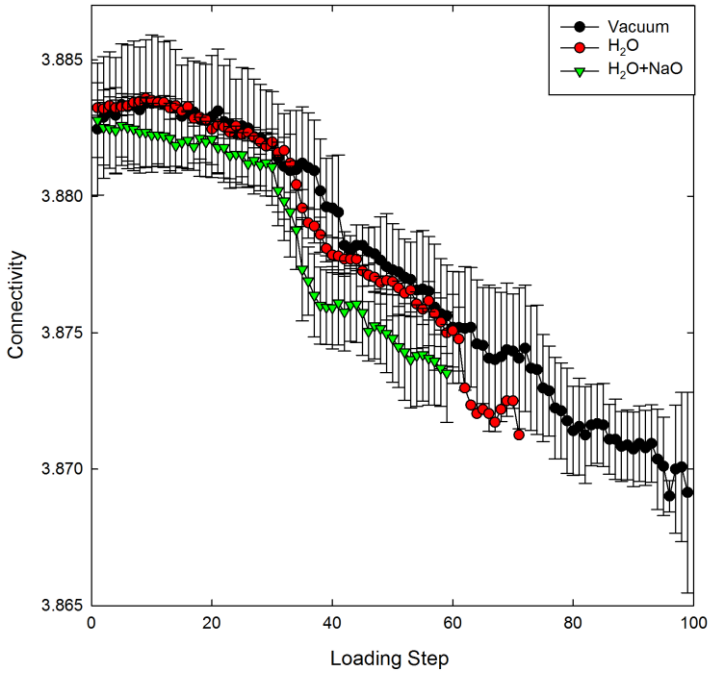

Changing connectivity of the silica during loading in three different environments

Crack tip shape

Sandia National Laboratories

	Dry	Hydrated (H_2O)	Hydrated (H_2O+Na)
Loading Steph = 25	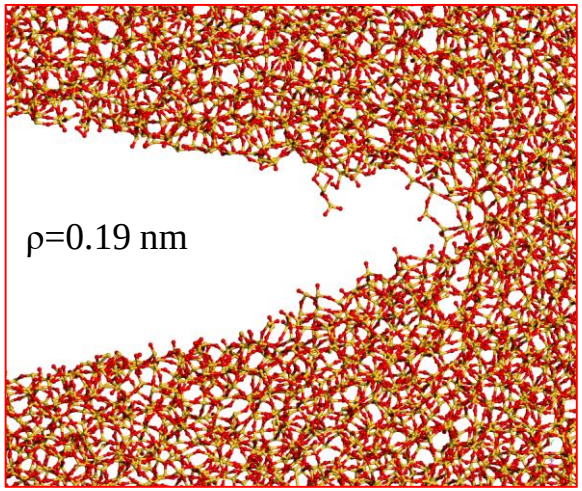 ρ=0.19 nm	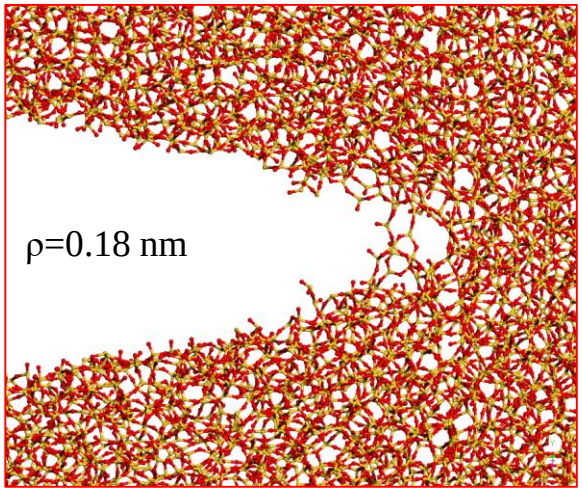 ρ=0.18 nm	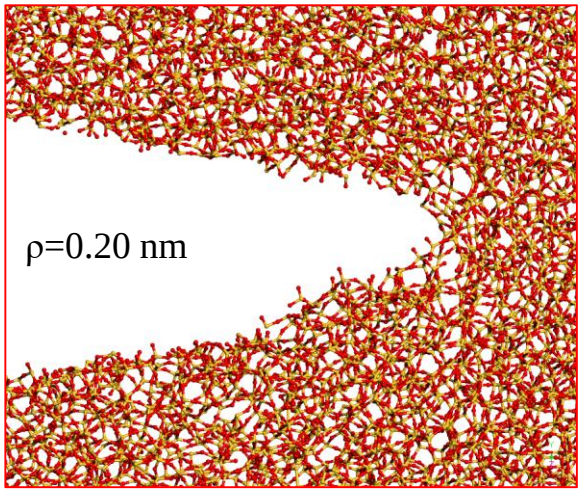 ρ=0.20 nm
Loading Steph = 75	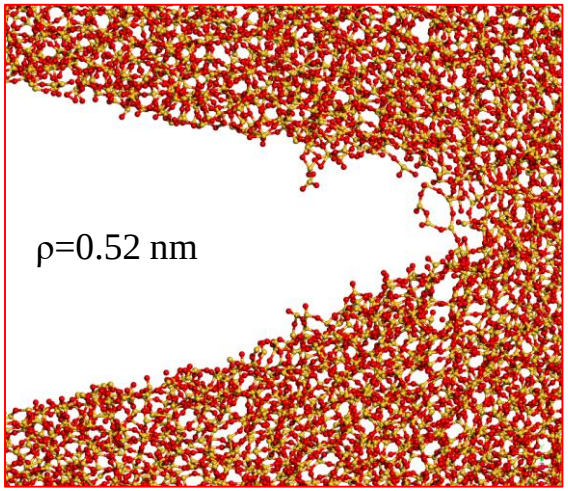 ρ=0.52 nm	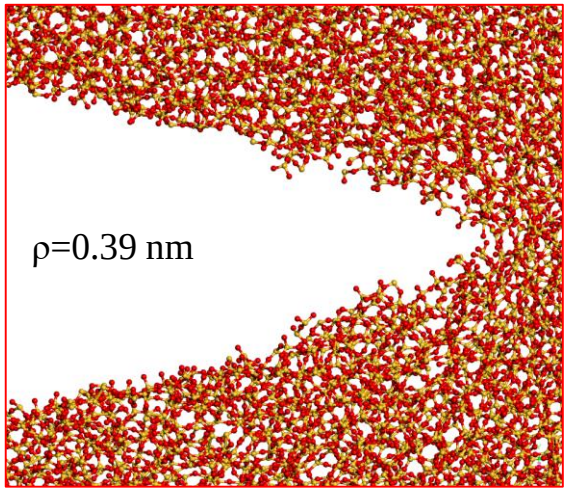 ρ=0.39 nm	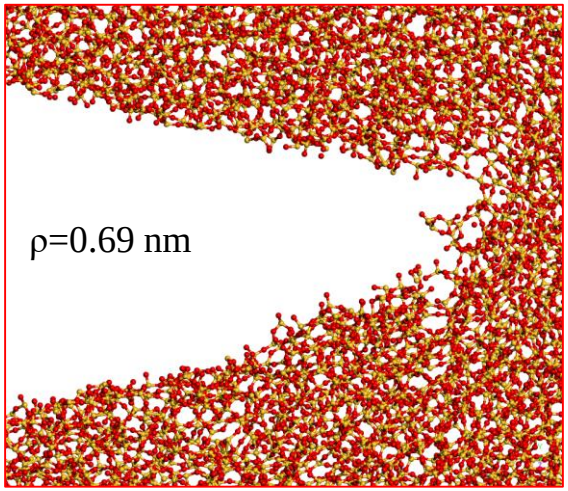 ρ=0.69 nm

Conclusions

- Dry silica fracture:
  - Development of localized high stress inelastic region prior to fracture
  - Inelastic zone estimated with a radius between 3-3.2 nm
  - K_{IC} of ~0.78 MPa$\sqrt{m}$ consistent with experimental results
- Atoms-to-Continuum methods appropriate for evaluating macroscopic fracture properties from atomistic scale information
- Hydrated silica fracture:
  - Decreasing connectivity of the structure during crack propagation
  - Changing morphology of the crack tip

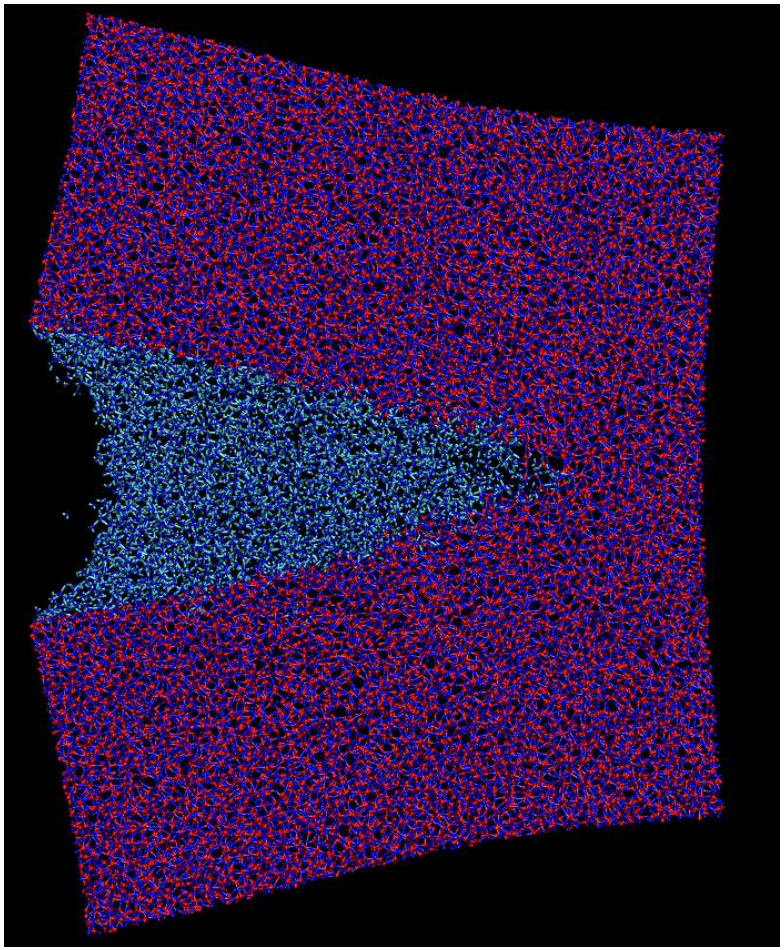

Snapshot of fracture silica in a hydrated environment

Ongoing work related to fracture

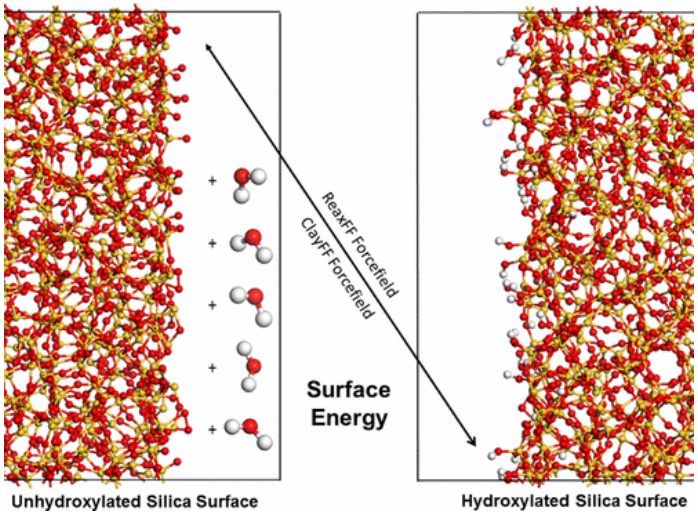

Rimsza, J. M., R. E. Jones, and L. J. Criscenti. "Surface structure and stability of partially hydroxylated silica surfaces." *Langmuir* 33.15 (2017): 3882-3891.

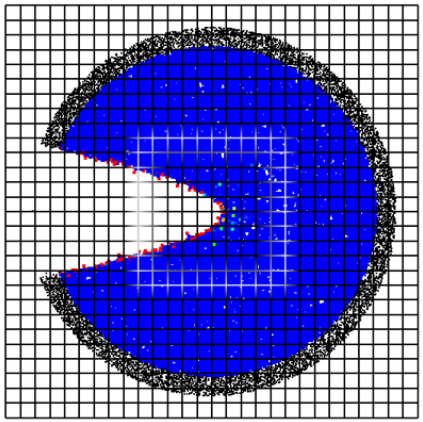

Atoms colored by PE, notice significant surface energy

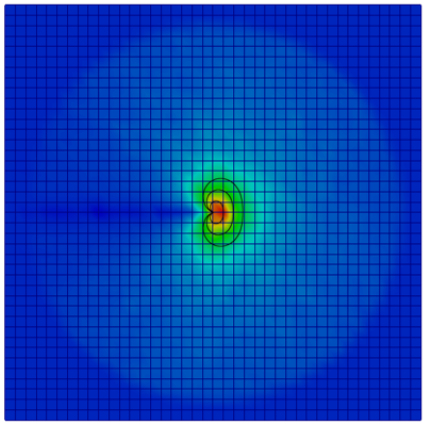

Coarse-grained energy density (color) corresponds well to theory (contours)

R. E. Jones, J.M. Rimsza, and L. J. Criscenti. "At atomic-scale evaluation of the fracture toughness of silica glass" *In preparation*

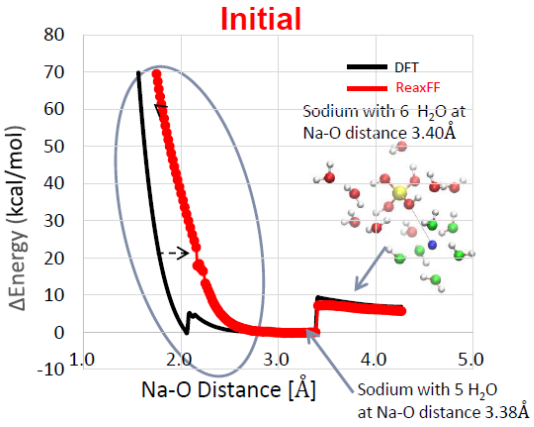

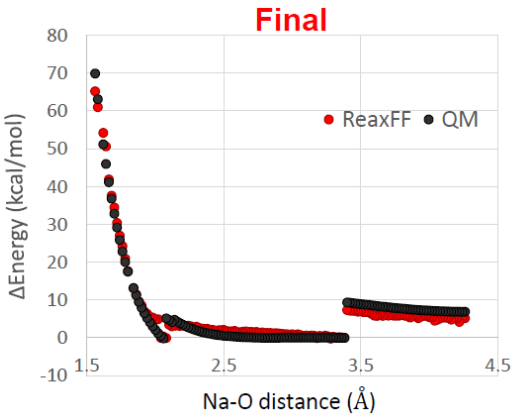

Seung Ho, J.M. Rimsza, L. J. Criscenti, ACT van Duin et al. "Silica dissolution in electrolyte solutions by ReaxFF classical MD simulations " *In preparation*

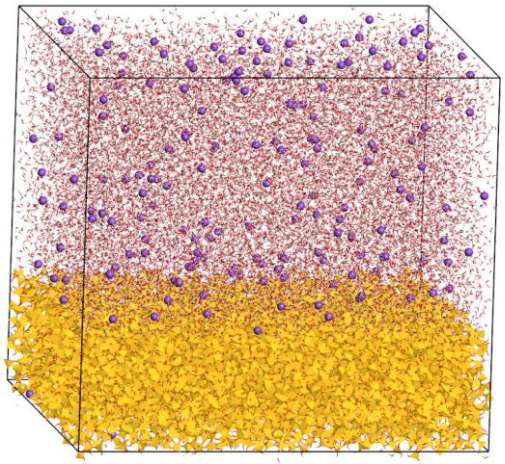

J.M. Rimsza, R.E. Jones, and L.J. Criscenti "Sodium Adsorption on Silica Surfaces " *In preparation*

Plasma bombardment of organosilicates

- Low-k dielectrics used in microelectronics
- Copper is added by removing low-k dielectrics by plasma bombardment
- Investigate stability by molecular simulation

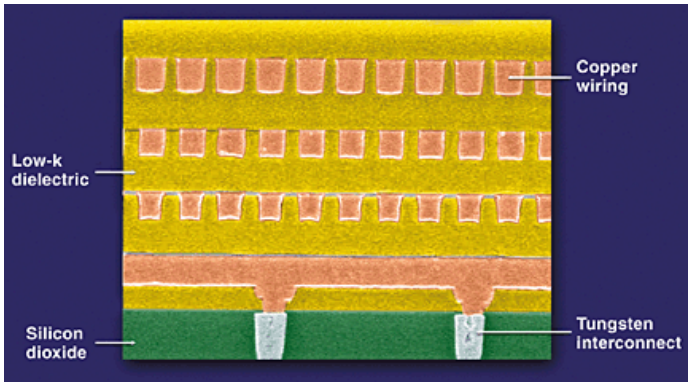

http://pubs.acs.org/cen/coverstory/7847/print/7847bus1.html

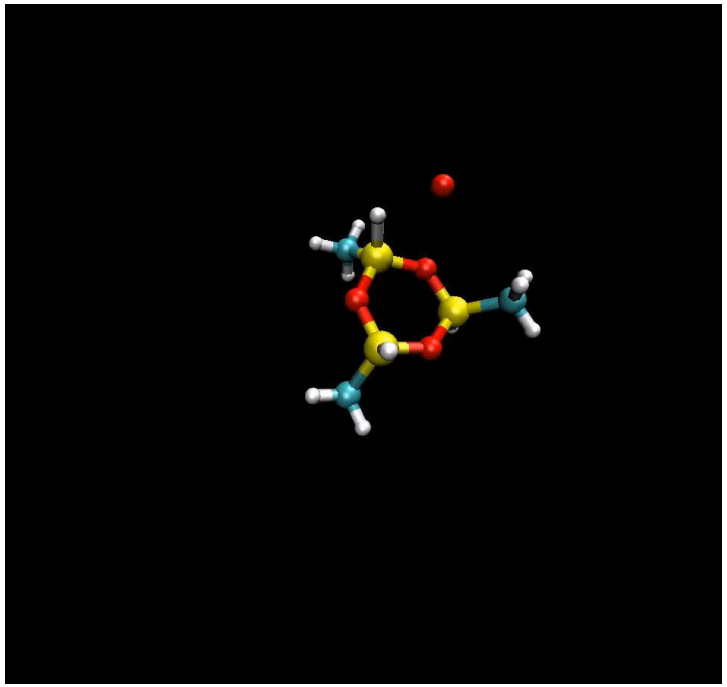

Rimsza, J. M. et. al. *J. Phys. D: Appl. Phys.* (2014)

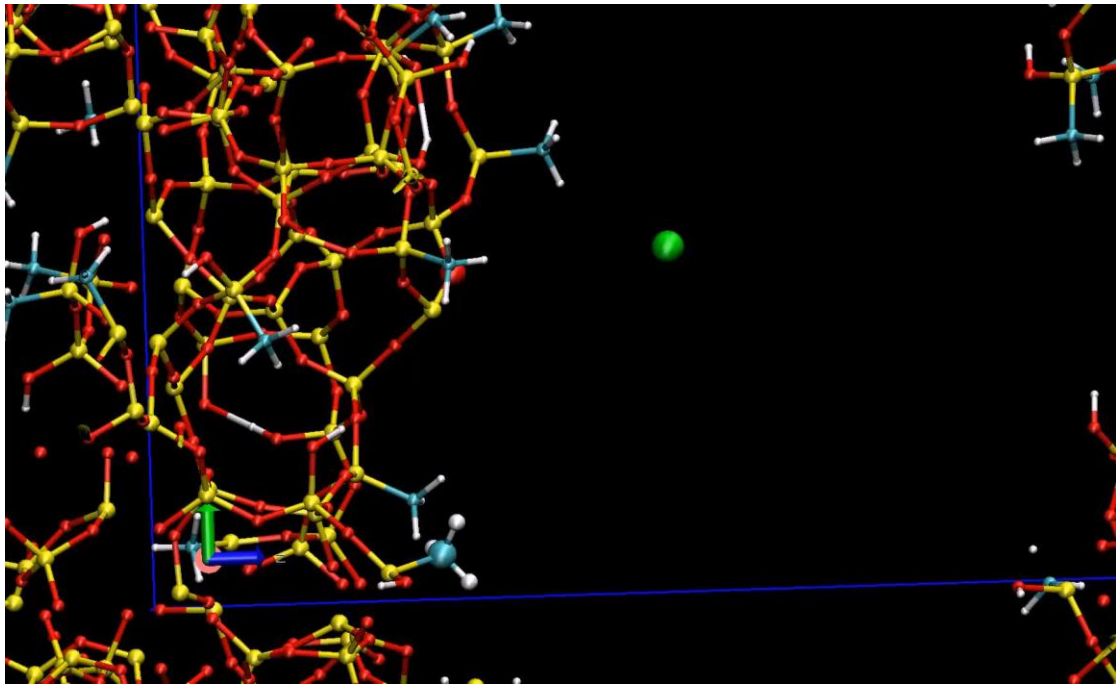

Rimsza, J. M., and Jincheng Du. *Comp. Mat. Sci.* (2015)

Sandia National Laboratories

Thank you for your attention!

Dissolution of Amorphous Silica

Jessica M. Rimsza (SNL) Jincheng Du (UNT), Jeffrey Kelber (UNT), Lu Deng (UNT), Haseeb Kazi, (UNT, Lam Research), Adri van Duin (Penn. St.), Jejoon Yun (Penn. St., U.C. Merced)

Fracture of Amorphous Silica

Jessica M. Rimsza (SNL) Louise Criscenti (SNL), Reese Jones (SNL), Adri van Duin (Penn. St.), Seung Ho (Penn. St.)

U.S. DEPARTMENT OF ENERGY

Crack tip blunting

- Crack tip blunting indicates an even stress distribution and local inelastic behavior
- Strength of a material is proportional to the radius of curvature of the crack tip (ρ):

$$\sigma_{max} \propto \sqrt{\frac{1}{\rho}}$$

C.E. Inglis, Spie Milestone series MS (1997)

- To calculate ρ the internal atoms of the crack tip are fit with a parabolic function, from which ρ is calculated:

A. Howard, Calculus: With analytic geometry, John Wiley 1988.

$$\rho = \frac{(1 + f'(x)^2)^{\frac{3}{2}}}{f''(x)}$$

- Radius of curvature: 0.1Å-5Å, experimental value: 15Å *Bando et al. J. Amer. Cera. Soc. 67.3 (1984).*
- Increasing stress around the crack tip prior to fracture
- Identifies size of the inelastic zone and development of a high stress conditions ahead of the crack tip

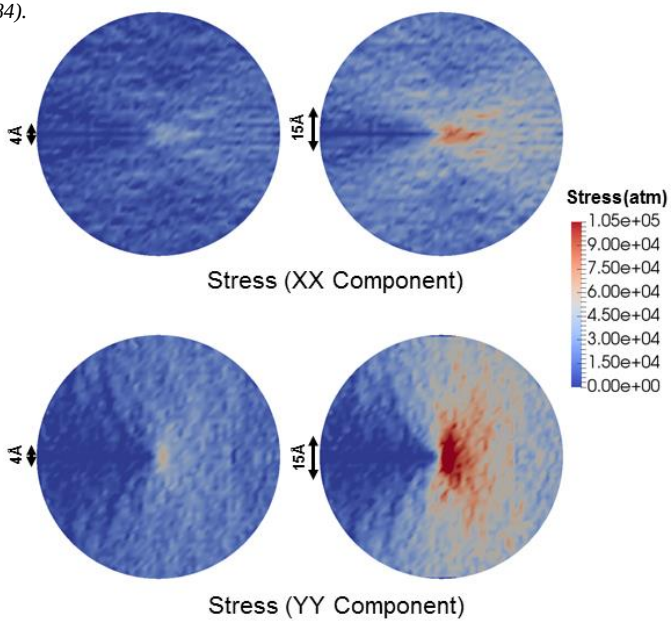

Stress fields calculated from individual atomic stresses. Averaged over twelve different trajectories.

Silica structure (red and yellow) atoms in quadratic fit (turquoise), parabola estimating the shape of the crack tip (silver), and horizontal axis (blue)

Radius of curvature and crack length during brittle fracture in silica